

Multi-fidelity Gaussian Process Bandit Optimisation

Kirthevasan Kandasamy[‡]

Gautam Dasarathy[‡]

Junier Oliva[‡]

Jeff Schneider[‡]

Barnabás Póczos[‡]

KANDASAMY@CS.CMU.EDU

GAUTAMD@RICE.EDU

JOLIVA@CS.CMU.EDU

SCHNEIDE@CS.CMU.EDU

BAPOCZOS@CS.CMU.EDU

[‡] Machine Learning Department, Carnegie Mellon University, Pittsburgh, PA 15213, USA

[‡] Electrical and Computer Engineering, Rice University, Houston, TX 77005, USA

Abstract

In many scientific and engineering applications, we are tasked with the optimisation of an expensive to evaluate black box function f . Traditional settings for this problem assume just the availability of this single function. However, in many cases, cheap approximations to f may be obtainable. For example, the expensive real world behaviour of a robot can be approximated by a cheap computer simulation. We can use these approximations to eliminate low function value regions cheaply and use the expensive evaluations of f in a small but promising region and speedily identify the optimum. We formalise this task as a *multi-fidelity* bandit problem where the target function and its approximations are sampled from a Gaussian process. We develop MF-GP-UCB, a novel method based on upper confidence bound techniques. In our theoretical analysis we demonstrate that it exhibits precisely the above behaviour, and achieves better regret than strategies which ignore multi-fidelity information. Empirically, MF-GP-UCB outperforms such naive strategies and other multi-fidelity methods on several synthetic and real experiments.

Keywords: Multi-fidelity optimisation, Bandits, Bandit Optimisation, Bayesian optimisation, Gaussian processes.

1. Introduction

In stochastic bandit optimisation, we wish to optimise a function $f : \mathcal{X} \rightarrow \mathbb{R}$ by sequentially querying it and obtaining *bandit feedback*, i.e. when we query at any $x \in \mathcal{X}$, we observe a possibly noisy evaluation of $f(x)$. f is typically expensive and the goal is to identify its maximum while keeping the number of queries as low as possible. Some applications are hyper-parameter tuning in expensive machine learning algorithms, optimal policy search in complex systems, and scientific experiments [Martinez-Cantin et al. \(2007\)](#); [Parkinson et al. \(2006\)](#); [Snoek et al. \(2012\)](#). Historically, bandit problems were studied in settings where the goal is to maximise the cumulative reward of all queries to the payoff instead of just finding the maximum. Applications in this setting include clinical trials and online advertising.

Conventional methods in these settings assume access to only this single expensive function of interest f . We will collectively refer to them as *single fidelity* methods. In many practical problems however, cheap approximations to f might be available. For instance, when tuning hyper-parameters of learning algorithms, the goal is to maximise a cross validation score on a training set, which can be expensive if the training set is large. However validation curves tend to vary smoothly with training set size; therefore, we can train and cross validate on small subsets to approximate the validation

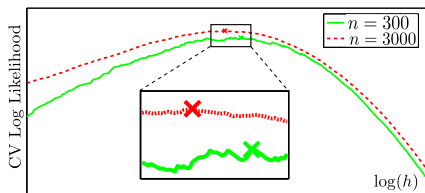


Figure 1: Average 5-fold cross validation log likelihood on datasets of size 300 and 3000 on a synthetic kernel density estimation task. The crosses are the maxima.

accuracies of the entire dataset. For a concrete example, consider kernel density estimation (KDE), where we need to tune the bandwidth h of a kernel. Figure 1 shows the average cross validation likelihood against h for a dataset of size $n = 3000$ and a smaller subset of size $n = 300$. Since the cross validation performance of a hyper-parameter depends on the training set size (Vapnik and Vapnik, 1998), we can only obtain a biased estimate of the cross validation performance with 3000 points using a subset of size 300. Consequently, the two maximisers are also different. That said, the curve for $n = 300$ approximates the $n = 3000$ curve quite well. Since training and cross validation on small n is cheap, we can use it to eliminate bad values of the hyper-parameters and reserve the expensive experiments with the entire dataset for the promising hyper-parameter values (e.g. boxed region in Figure 1).

In the conventional treatment for online advertising, each query to f is, say, the public display of an ad on the internet for a certain time period. However, we could also choose smaller experiments by, say, confining the display to a small geographic region and/or for shorter periods. The estimate is biased, since users in different geographies are likely to have different preferences, but will nonetheless be useful in gauging the all round performance of an ad. In optimal policy search in robotics and autonomous driving, vastly cheaper computer simulations are used to approximate the expensive real world performance of the system (Cutler et al., 2014; Urmson et al., 2008). Scientific experiments can be approximated to varying degrees using less expensive data collection, analysis, and computational techniques (Parkinson et al., 2006).

In this paper, we cast these tasks as *multi-fidelity bandit optimisation* problems assuming the availability of cheap approximate functions (fidelities) to the payoff f . **Our contributions** are:

1. We present a formalism for multi-fidelity bandit optimisation using Gaussian process (GP) assumptions on f and its approximations. We develop a novel algorithm, Multi-Fidelity Gaussian Process Upper Confidence Bound (MF-GP-UCB) for this setting.
2. Our theoretical analysis proves that MF-GP-UCB explores the space \mathcal{X} at lower fidelities and uses the high fidelities in successively smaller regions to converge on the optimum. As lower fidelity queries are cheaper, MF-GP-UCB has better regret than single fidelity strategies which have to rely on the expensive function to explore the entire space.
3. We demonstrate that MF-GP-UCB outperforms single fidelity methods and other alternatives empirically, via a series of synthetic examples, three hyper-parameter tuning tasks and one inference problem in astrophysics. Our matlab implementation and experiments are available at github.com/kirthevasank/mf-gp-ucb.

Related Work

Since the seminal work by Robbins (1952), the multi-armed bandit problem has been studied extensively in the K -armed setting. Recently, there has been a surge of interest in the optimism under uncertainty principle for K -armed bandits, typified by upper confidence bound (UCB) methods (Auer,

2003; Bubeck and Cesa-Bianchi, 2012). UCB strategies have also been used in bandit tasks with linear (Dani et al., 2008) and GP (Srinivas et al., 2010) payoffs. There is a plethora of work on single fidelity methods for global optimisation both with noisy and noiseless evaluations. Some examples are branch and bound techniques such as dividing rectangles (DiRect) Jones et al. (1993), simulated annealing, genetic algorithms and more Kawaguchi et al. (2015); Kirkpatrick et al. (1983); Munos (2011). A suite of single fidelity methods in the GP framework closely related to our work is Bayesian Optimisation (BO). While there are several techniques for BO (Hernández-Lobato et al., 2014; Jones et al., 1998; Mockus, 1994; Thompson, 1933), of particular interest to us is the Gaussian process upper confidence bound (GP-UCB) algorithm of Srinivas et al. (2010).

Many applied domains of research such as aerodynamics, industrial design and hyper-parameter tuning have studied multi-fidelity methods (Forrester et al., 2007; Huang et al., 2006; Klein et al., 2015; Swersky et al., 2013); a plurality of them use BO techniques. However none of these treatments neither formalise nor analyse any notion of *regret* in the multi-fidelity setting. In contrast, MF-GP-UCB is an intuitive UCB idea with good theoretical properties. Agarwal et al. (2011) derive oracle inequalities for hyper-parameter tuning with ERM under computational budgets. Our setting is more general as it applies to any bandit optimisation task. Sabharwal et al. (2015) present a UCB based idea for tuning hyper-parameters with incremental data allocation. However, their theoretical results are for an idealised non-realizable algorithm. Cutler et al. (2014) study reinforcement learning with multi-fidelity simulators by treating each fidelity as a Markov Decision Process. Finally, Zhang and Chaudhuri (2015) study active learning when there is access to a cheap weak labeler and an expensive strong labeler. The latter set of work above study problems different to optimisation.

Recently, in Kandasamy et al. (2016b) we studied the classical K -armed bandit in multi-fidelity settings. Here, we build on this work to study multi-fidelity Bayesian optimisation; as such, we share similarities in the assumptions, algorithm and some analysis techniques. A preliminary version of this paper appeared in Kandasamy et al. (2016a) where we provided theoretical results in continuous domains and with two fidelities (one approximation). Here, we also analyse the discrete domains and present results for a general number of fidelities. Furthermore, we eliminate some technical assumptions from our previous work and present cleaner and more interpretable versions of our theorems. In follow up work (Kandasamy et al., 2017), we extend multi-fidelity optimisation to settings with continuous approximations. While the assumptions there are considerably different, it builds on the main intuitions from this work. To the best of our knowledge, this is the first line of work to formalise a notion of regret and provide a theoretical analysis for multi-fidelity optimisation.

The remainder of this manuscript is organised as follows. Section 2 presents our formalism including a notion of simple regret for multi-fidelity GP optimisation. Section 4 presents our algorithm. We present our theoretical results in Section 5 beginning with an informal discussion of results for $M = 2$ fidelities in Section 5.1 to elucidate their main ideas. The proofs are given in Section 8. Section 7 presents our experiments with some details deferred to Appendix A. Appendix B collects some ancillary material including a table of notations and abbreviations in Appendix B.2.

2. Problem Set Up

We wish to maximise a function $f : \mathcal{X} \rightarrow \mathbb{R}$ where \mathcal{X} is a (possibly finite and/or discrete) compact subset of $[0, r]^d$, where $r > 0$ and d is the dimension of \mathcal{X} . We can interact with f only by querying it at some $x \in \mathcal{X}$ and obtaining a noisy evaluation $y = f(x) + \epsilon$ of f , where the noise satisfies $\mathbb{E}[\epsilon] = 0$. Let $x_* \in \operatorname{argmax}_{x \in \mathcal{X}} f(x)$ be a maximiser of f and $f_* = f(x_*)$ be the maximum value.

Let $x_t \in \mathcal{X}$ be the point queried at time t by a sequential procedure. Our goal in bandit optimisation is to achieve small *simple regret* S_n , defined below, after n queries to f .

$$S_n = \min_{t=1, \dots, n} f_\star - f(x_t). \quad (1)$$

Our primary distinction from the usual setting is that we have access to $M - 1$ successively accurate approximations $f^{(1)}, f^{(2)}, \dots, f^{(M-1)}$ to the function of interest $f = f^{(M)}$. We refer to these approximations as fidelities. The multi-fidelity framework is attractive when the following two conditions are true about the problem.

1. *The approximations $f^{(1)}, \dots, f^{(M-1)}$ approximate $f^{(M)}$.* To this end, we will assume a uniform bound for the fidelities, $\|f^{(M)} - f^{(m)}\|_\infty \leq \zeta^{(m)}$ for $m = 1, \dots, M$, where the bounds $\zeta^{(1)} > \zeta^{(2)} > \dots > \zeta^{(M)} = 0$ are known.
2. *There approximations are cheaper than evaluating at $f^{(M)}$.* We will assume that a query at fidelity m expends a cost $\lambda^{(m)}$ of a resource, e.g. computational effort or money. The costs are known and satisfy $0 < \lambda^{(1)} < \lambda^{(2)} < \dots < \lambda^{(M)}$.

Therefore, as the fidelity m increases, the approximations become better but are also more costly. An algorithm for multi-fidelity bandits is a sequence of query-fidelity pairs $\{(x_t, m_t)\}_{t \geq 0}$, where at time n , the algorithm chooses (x_n, m_n) using information from previous query-observation-fidelity triples $\{(x_t, y_t, m_t)\}_{t=1}^{n-1}$. Here $y_t = f^{(m_t)}(x_t) + \epsilon_t$ where, $\mathbb{E}[\epsilon_t] = 0$.

Some smoothness assumptions on $f^{(m)}$'s are needed to make the problem tractable. A standard in the Bayesian nonparametric literature is to use a Gaussian process (GP) prior (Rasmussen and Williams, 2006) with covariance kernel κ . Two popular kernels of choice are the squared exponential (SE) kernel $\kappa_{\sigma, h}$ and the Matérn kernel $\kappa_{\nu, \rho}$. Writing $z = \|x - x'\|_2$, they are defined as

$$\kappa_{\sigma, h}(x, x') = \sigma \exp\left(-\frac{z^2}{2h^2}\right), \quad \kappa_{\nu, \rho}(x, x') = \frac{2^{1-\nu}}{\Gamma(\nu)} \left(\frac{\sqrt{2\nu}z}{\rho}\right)^\nu B_\nu\left(\frac{\sqrt{2\nu}z}{\rho}\right),$$

respectively. Here $\sigma, h, \nu, \rho > 0$ are parameters of the kernels and Γ, B_ν are the Gamma and modified Bessel functions. A convenience the GP framework offers is that posterior distributions are analytically tractable. If $f \sim \mathcal{GP}(0, \kappa)$ is a sample from a GP, and we have observations $\mathcal{D}_n = \{(x_i, y_i)\}_{i=1}^n$, where $y_i = f(x_i) + \epsilon$ and $\epsilon \sim \mathcal{N}(0, \eta^2)$ is Gaussian noise, then the posterior distribution for $f(x) | \mathcal{D}_n$ is also Gaussian $\mathcal{N}(\mu_n(x), \sigma_n^2(x))$ with

$$\mu_n(x) = k^\top (K + \eta^2 I_n)^{-1} Y, \quad \sigma_n^2(x) = \kappa(x, x) - k^\top (K + \eta^2 I_n)^{-1} k. \quad (2)$$

Here, $Y \in \mathbb{R}^n$ is a vector with $Y_i = y_i$, $k \in \mathbb{R}^n$ is a vector with $k_i = \kappa(x, x_i)$. The matrix $K \in \mathbb{R}^{n \times n}$ is given by $K_{i,j} = \kappa(x_i, x_j)$. $I_n \in \mathbb{R}^{n \times n}$ is the $n \times n$ identity matrix. In keeping with the above framework, we make the following assumptions on our problem.

- A1. (GP Assumption)** $f^{(m)} \sim \mathcal{GP}(0, \kappa)$ for all $m = 1, \dots, M$. Upon querying $f^{(m)}$ at x_t we observe $f^{(m)}(x_t) + \epsilon$ where $\epsilon \sim \mathcal{N}(0, \eta^2)$ is Gaussian noise with variance η^2 .
- A2. (Multi-fidelity Assumption)** $\|f^{(M)} - f^{(m)}\|_\infty \leq \zeta^{(m)}$ for all $m = 1, \dots, M$, where the bounds $\zeta^{(1)} > \zeta^{(2)} > \dots > \zeta^{(M)} = 0$ are known.

In Remark 16, Appendix B.1 we argue that assumption A2 continues to hold with nontrivial probability when we sample $f^{(m)}$'s from a GP. So a generative mechanism would keep sampling the functions and deliver them when the conditions hold true. Assumption A1 can be relaxed to hold for different kernels and noise variances for each fidelity, i.e different $\kappa^{(m)}, \eta^{(m)}$ for $m = 1, \dots, M$, with minimal modifications to our analysis but we use the above form to simplify the presentation of the results. In fact, our practical implementation uses different kernels.

Simple Regret for Multi-fidelity Optimisation: Our goal is to achieve small simple regret $S(\Lambda)$ after spending capital Λ of a resource. We will aim to provide *any-capital* bounds, meaning that we will assume that the game is played indefinitely and will try to bound the regret for all (sufficiently large) values of Λ . This is similar in spirit to any-time analyses in single fidelity bandit methods as opposed to fixed time horizon analyses. Let $\{m_t\}_{t \geq 0}$ be the fidelities queried by a multi-fidelity method at each time step. Let N be the *random* quantity such that $N = \max\{n \geq 1 : \sum_{t=1}^n \lambda^{(m_t)} \leq \Lambda\}$, i.e. it is number of queries the strategy makes across all fidelities until capital Λ . Only the optimum of $f = f^{(M)}$ is of interest to us. The lower fidelities are useful to the extent that they help us optimise $f^{(M)}$ with less cost, but there is no reward for optimising a cheaper approximation. Accordingly, we set the instantaneous reward q_t at time t to be $-\infty$ if $m_t \neq M$ and $f^{(M)}(x_t)$ if $m_t = M$. If we let $r_t = f_\star - q_t$ denote the instantaneous regret, we have $r_t = +\infty$ if $m_t \neq M$ and $f_\star - f^{(M)}(x_t)$ if $m_t = M$. For optimisation, the simple regret is simply the best instantaneous regret, $S(\Lambda) = \min_{t=1, \dots, N} r_t$. Equivalently,

$$S(\Lambda) = \min_{t=1, \dots, N} r_t = \begin{cases} \min_{\substack{t=1, \dots, N \\ t: m_t=M}} f_\star - f^{(M)}(x_t) & \text{if we have queried at the } M^{\text{th}} \text{ fidelity} \\ & \text{at least once,} \\ +\infty & \text{otherwise.} \end{cases} \quad (3)$$

Note that the above reduces to S_n in (1) when we only have access to $f^{(M)}$ with $n = N = \lfloor \Lambda / \lambda^{(M)} \rfloor$.

Before we proceed, we note that it is customary in the bandit literature to analyse *cumulative regret*. The definition of cumulative regret depends on the application at hand (Kandasamy et al., 2016b) and our results can be extended to many sensible notions of cumulative regret. However, both to simplify exposition and since our focus in this paper is optimisation, we stick to simple regret.

Challenges: We conclude this section with a commentary on some of the challenges in multi-fidelity optimisation using Figure 2 for illustration. For simplicity, we will focus on 2 fidelities when we have one approximation $f^{(1)}$ to an expensive function $f^{(2)}$. For now assume that (unrealistically) $f^{(1)}$ and its optimum $x_\star^{(1)}$ are known. Typically $x_\star^{(1)}$ is suboptimal for $f^{(2)}$. A seemingly straightforward solution might be to search for x_\star in an appropriate subset, such as a neighborhood of $x_\star^{(1)}$. However, if this neighborhood is too small, we might miss the optimum x_\star (green region in Figure 2(a)). A crucial challenge for multi-fidelity methods is to not get stuck at the optimum of a lower fidelity. While exploiting information from lower fidelities, it is also important to *explore* sufficiently at higher fidelities. In our experiments we demonstrate that naive strategies which do not do so would get stuck at the optimum of a lower fidelity. Alternatively, if we pick a very large subset (Figure 2(b)) we might not miss x_\star ; however, it defeats the objectives of the multi-fidelity set up where the goal is to use the approximation to be prudent about where we query $f^{(2)}$. Figure 2(c) seems like a sensible subset, but it remains to be seen how it is chosen. Further, this subset might not even be a neighborhood as illustrated in Figure 2(d), where $f^{(1)}, f^{(2)}$ are multi-modal and the optima are in different modes.

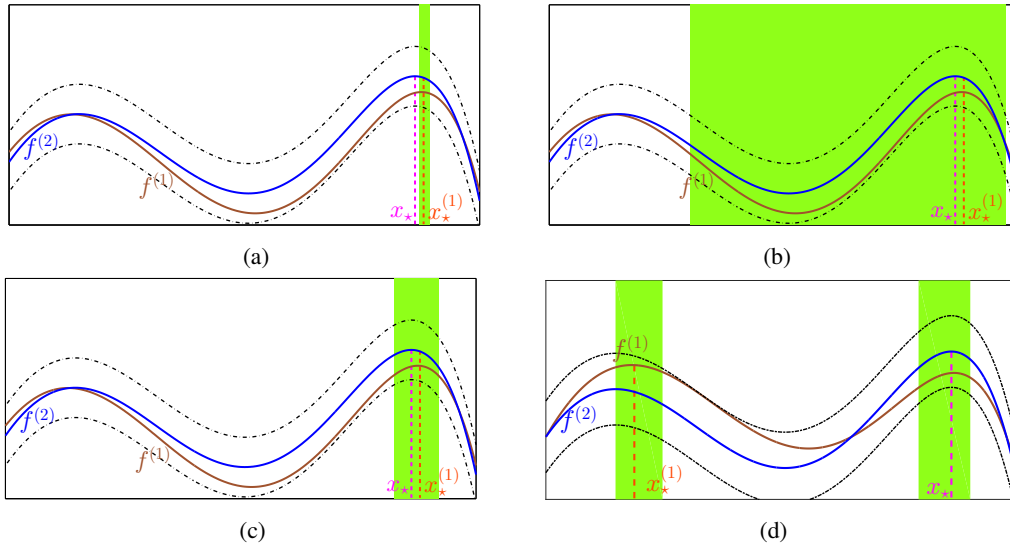


Figure 2: An illustration of the challenges in multi-fidelity optimisation. See main text.

In such cases, an appropriate algorithm should explore all such modes. On top of the above, an algorithm does not actually know $f^{(1)}$. A sensible algorithm should explore $f^{(1)}$ and simultaneously identify the above subset, either implicitly or explicitly, for exploration at the second fidelity $f^{(2)}$.

3. A Review of GP-UCB

Sequential optimisation methods adopting UCB principles maintain a high probability upper bound $\varphi_t : \mathcal{X} \rightarrow \mathbb{R}$ for $f(x)$ for all $x \in \mathcal{X}$ (Auer, 2003). At time t we query at the maximiser of this upper bound $x_t = \operatorname{argmax}_{x \in \mathcal{X}} \varphi_t(x)$. Our work builds on GP-UCB (Srinivas et al., 2010), where φ_t takes the form $\varphi_t(x) = \mu_{t-1}(x) + \beta_t^{1/2} \sigma_{t-1}(x)$. Here μ_{t-1}, σ_{t-1} are the posterior mean and standard deviation of the GP conditioned on the previous $t - 1$ queries $\{(x_i, y_i)\}_{i=1}^{t-1}$. The key intuition here is that the mean μ_{t-1} encourages an exploitative strategy – in that we want to query where we know the function is high – and the confidence band $\beta_t^{1/2} \sigma_{t-1}$ encourages an explorative strategy – in that we want to query at regions we are uncertain about f lest we miss out on high valued regions. We have presented GP-UCB in Algorithm 1 and illustrated it in Figure 3.

Algorithm 1 GP-UCB (Srinivas et al., 2010)

Input: kernel κ .

- $\mathcal{D}_0 \leftarrow \emptyset, (\mu_0, \sigma_0) \leftarrow (\mathbf{0}, \kappa^{1/2})$.
 - **for** $t = 1, 2, \dots$
 1. $x_t \leftarrow \operatorname{argmax}_{x \in \mathcal{X}} \mu_{t-1}(x) + \beta_t^{1/2} \sigma_{t-1}(x)$
 2. $y_t \leftarrow$ Query f at x_t .
 3. Perform Bayesian posterior updates to obtain μ_t, σ_t . See (2).
-

To present the theoretical results for GP-UCB, we begin by defining the *Maximum Information Gain* (MIG) which characterises the statistical difficulty of GP bandits.

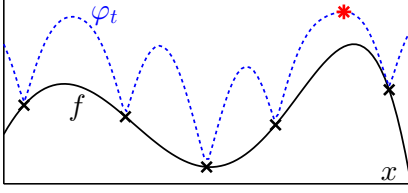


Figure 3: Illustration of GP-UCB. The solid black line is f . The dashed blue line is $\varphi_t = \mu_{t-1} + \beta_t^{1/2} \sigma_{t-1}$ which upper bounds f with high probability. The observations until $t-1$ are shown as black crosses. At time t , we query at the maximiser $x_t = \operatorname{argmax}_{x \in \mathcal{X}} \varphi_t(x)$ (red star).

Definition 1 (*Maximum Information Gain (Srinivas et al., 2010)*) Let $f \sim \mathcal{GP}(\mathbf{0}, \kappa)$. Consider any $A \subset \mathbb{R}^d$ and let $\tilde{A} = \{x_1, \dots, x_n\} \subset A$ be a finite subset. Let $f_{\tilde{A}}, \epsilon_{\tilde{A}} \in \mathbb{R}^n$ such that $(f_{\tilde{A}})_i = f(x_i)$, $(\epsilon_{\tilde{A}})_i \sim \mathcal{N}(0, \eta^2)$, and $y_{\tilde{A}} = f_{\tilde{A}} + \epsilon_{\tilde{A}}$. Let I denote the Shannon mutual information. The Maximum Information Gain $\Psi_n(A)$ of A after n evaluations is the maximum mutual information between the function values and observations among all choices of n points in A . Precisely,

$$\Psi_n(A) = \max_{\tilde{A} \subset A, |\tilde{A}|=n} I(y_{\tilde{A}}; f_{\tilde{A}}).$$

The MIG, which depends on the kernel and the set A , will be an important quantity in our analysis. For a given kernel it typically scales with the volume of A . For e.g. if $A = [0, r]^d$ then $\Psi_n(A) \in \mathcal{O}(r^d \Psi_n([0, 1]^d))$. It is known that for the SE kernel, $\Psi_n([0, 1]^d) \in \mathcal{O}((\log(n))^{d+1})$ and for the Matérn kernel, $\Psi_n([0, 1]^d) \in \mathcal{O}(n^{\frac{d(d+1)}{2\nu+d(d+1)}} \log(n))$ (Seeger et al., 2008; Srinivas et al., 2010). Next, we will need the following regularity conditions on the kernel. It is satisfied for four times differentiable kernels such as the SE kernel and Matérn kernel when $\nu > 2$ (Ghosal and Roy, 2006).

Assumption 2 Let $f \sim \mathcal{GP}(\mathbf{0}, \kappa)$, where $\kappa : [0, r]^d \times [0, r]^d \rightarrow \mathbb{R}$ is a stationary kernel (Rasmussen and Williams, 2006). The partial derivatives of f satisfies the following condition. There exist constants $a, b > 0$ such that,

$$\text{for all } J > 0, \text{ and for all } i \in \{1, \dots, d\}, \quad \mathbb{P} \left(\sup_x \left| \frac{\partial f(x)}{\partial x_i} \right| > J \right) \leq a e^{-(J/b)^2}.$$

The following theorem from Srinivas et al. (2010) bounds the simple regret S_n (1) for GP-UCB.

Theorem 3 (*Theorems 1 and 2 in Srinivas et al. (2010)*) Let $f \sim \mathcal{GP}(\mathbf{0}, \kappa)$, $f : \mathcal{X} \rightarrow \mathbb{R}$ and the kernel κ satisfies Assumption 2). At each query, we have noisy observations $y = f(x) + \epsilon$ where $\epsilon \sim \mathcal{N}(0, \eta^2)$. Denote $C_1 = 8 / \log(1 + \eta^{-2})$. Pick a failure probability $\delta \in (0, 1)$. The following bounds on the simple regret S_n hold with probability $> 1 - \delta$ for all $n \geq 1$.

- If \mathcal{X} is a finite discrete set, run GP-UCB with $\beta_t = 2 \log(|\mathcal{X}| t^2 \pi^2 / 6\delta)$. Then,

$$\text{for all } n \geq 1, \quad S_n \leq \sqrt{\frac{C_1 \beta_n \Psi_n(\mathcal{X})}{n}}$$

- If $\mathcal{X} = [0, r]^d$, run GP-UCB with $\beta_t = 2 \log\left(\frac{2\pi^2 t^2}{3\delta}\right) + 2d \log\left(t^2 b d r \sqrt{\frac{4ad}{\delta}}\right)$. Then,

$$\text{for all } n \geq 1, \quad S_n \leq \sqrt{\frac{C_1 \beta_n \Psi_n(\mathcal{X})}{n}} + 2$$

4. Multi-fidelity Gaussian Process Upper Confidence Bound (MF-GP-UCB)

We now propose MF-GP-UCB, which extends GP-UCB to the multi-fidelity setting. Like GP-UCB, MF-GP-UCB will also maintain a UCB for $f^{(M)}$ obtained via the previous queries at *all* fidelities. Denote the posterior GP mean and standard deviation of $f^{(m)}$ conditioned *only* on the previous queries at fidelity m by $\mu_t^{(m)}, \sigma_t^{(m)}$ respectively (See (2)). Then define,

$$\varphi_t^{(m)}(x) = \mu_{t-1}^{(m)}(x) + \beta_t^{1/2} \sigma_{t-1}^{(m)}(x) + \zeta^{(m)}, \quad \forall m, \quad \varphi_t(x) = \min_{m=1, \dots, M} \varphi_t^{(m)}(x). \quad (4)$$

For appropriately chosen β_t , $\mu_{t-1}^{(m)}(x) + \beta_t^{1/2} \sigma_{t-1}^{(m)}(x)$ will upper bound $f^{(m)}(x)$ with high probability. By **A2**, $\varphi_t^{(m)}(x)$ upper bounds $f^{(M)}(x)$ for all m . We have M such bounds, and their minimum $\varphi_t(x)$ gives the best upper bound for $f^{(M)}$. Following UCB strategies such as GP-UCB, our next query is at the maximiser of this UCB, $x_t = \operatorname{argmax}_{x \in \mathcal{X}} \varphi_t(x)$.

Next we need to decide which fidelity to query at. Consider any $m < M$. The $\zeta^{(m)}$ conditions on $f^{(m)}$ constrain the value of $f^{(M)}$ – the confidence band $\beta_t^{1/2} \sigma_{t-1}^{(m)}$ for $f^{(m)}$ is lengthened by $\zeta^{(m)}$ to obtain confidence on $f^{(M)}$. If $\beta_t^{1/2} \sigma_{t-1}^{(m)}(x_t)$ for $f^{(m)}$ is large, it means that we have not constrained $f^{(m)}$ sufficiently well at x_t and should query at the m^{th} fidelity. On the other hand, querying indefinitely in the same region to reduce the uncertainty $\beta_t^{1/2} \sigma_{t-1}^{(m)}$ at the m^{th} fidelity in that region will not help us much as the $\zeta^{(m)}$ elongation caps off how much we can learn about $f^{(M)}$ from $f^{(m)}$; i.e. even if we knew $f^{(m)}$ perfectly, we will only have constrained $f^{(M)}$ to within a $\pm \zeta^{(m)}$ band. Our algorithm captures this simple intuition. Having selected x_t , we begin by checking at the first fidelity. If $\beta_t^{1/2} \sigma_{t-1}^{(1)}(x_t)$ is smaller than a threshold $\gamma^{(1)}$, we proceed to the second fidelity. If at any stage $\beta_t^{1/2} \sigma_{t-1}^{(m)}(x_t) \geq \gamma^{(m)}$ we query at fidelity $m_t = m$. If we proceed all the way to fidelity M , we query at $m_t = M$. We will discuss choices for $\gamma^{(m)}$ in Sections 5.1 and 6. We summarise the resulting procedure in Algorithm 2.

Algorithm 2 MF-GP-UCB

Inputs: kernel κ , bounds $\{\zeta^{(m)}\}_{m=1}^M$, thresholds $\{\gamma^{(m)}\}_{m=1}^M$.

- For $m = 1, \dots, M$: $\mathcal{D}_0^{(m)} \leftarrow \emptyset$, $(\mu_0^{(m)}, \sigma_0^{(m)}) \leftarrow (\mathbf{0}, \kappa^{1/2})$.
 - for $t = 1, 2, \dots$
 1. $x_t \leftarrow \operatorname{argmax}_{x \in \mathcal{X}} \varphi_t(x)$. See (4) for φ_t and Sections 5, 6 for β_t .
 2. $m_t = \min_m \{m \mid \beta_t^{1/2} \sigma_{t-1}^{(m)}(x_t) \geq \gamma^{(m)} \text{ or } m = M\}$.
 3. $y_t \leftarrow \text{Query } f^{(m_t)} \text{ at } x_t$.
 4. Update $\mathcal{D}_t^{(m_t)} \leftarrow \mathcal{D}_{t-1}^{(m_t)} \cup \{(x_t, y_t)\}$. Obtain $\mu_t^{(m_t)}, \sigma_t^{(m_t)}$ conditioned on $\mathcal{D}_t^{(m_t)}$ (2).
Set $\mathcal{D}_t^{(m)} \leftarrow \mathcal{D}_{t-1}^{(m)}$, $\mu_t^{(m)} \leftarrow \mu_{t-1}^{(m)}$, $\sigma_t^{(m)} \leftarrow \sigma_{t-1}^{(m)}$ for $m \neq m_t$.
-

Before we proceed, we make an essential observation. The posterior for any $f^{(m)}(x)$ conditioned on previous queries at *all* fidelities $\bigcup_{\ell=1}^M \mathcal{D}_t^{(\ell)}$ is not Gaussian due to the $\zeta^{(m)}$ constraints (**A2**). However, $|f^{(m)}(x) - \mu_{t-1}^{(m)}(x)| < \beta_t^{1/2} \sigma_{t-1}^{(m)}(x)$ holds with high probability, since, by conditioning only on queries at the m^{th} fidelity we have Gaussianity for $f^{(m)}(x)$. (See Lemma 9, Appendix 8.1).

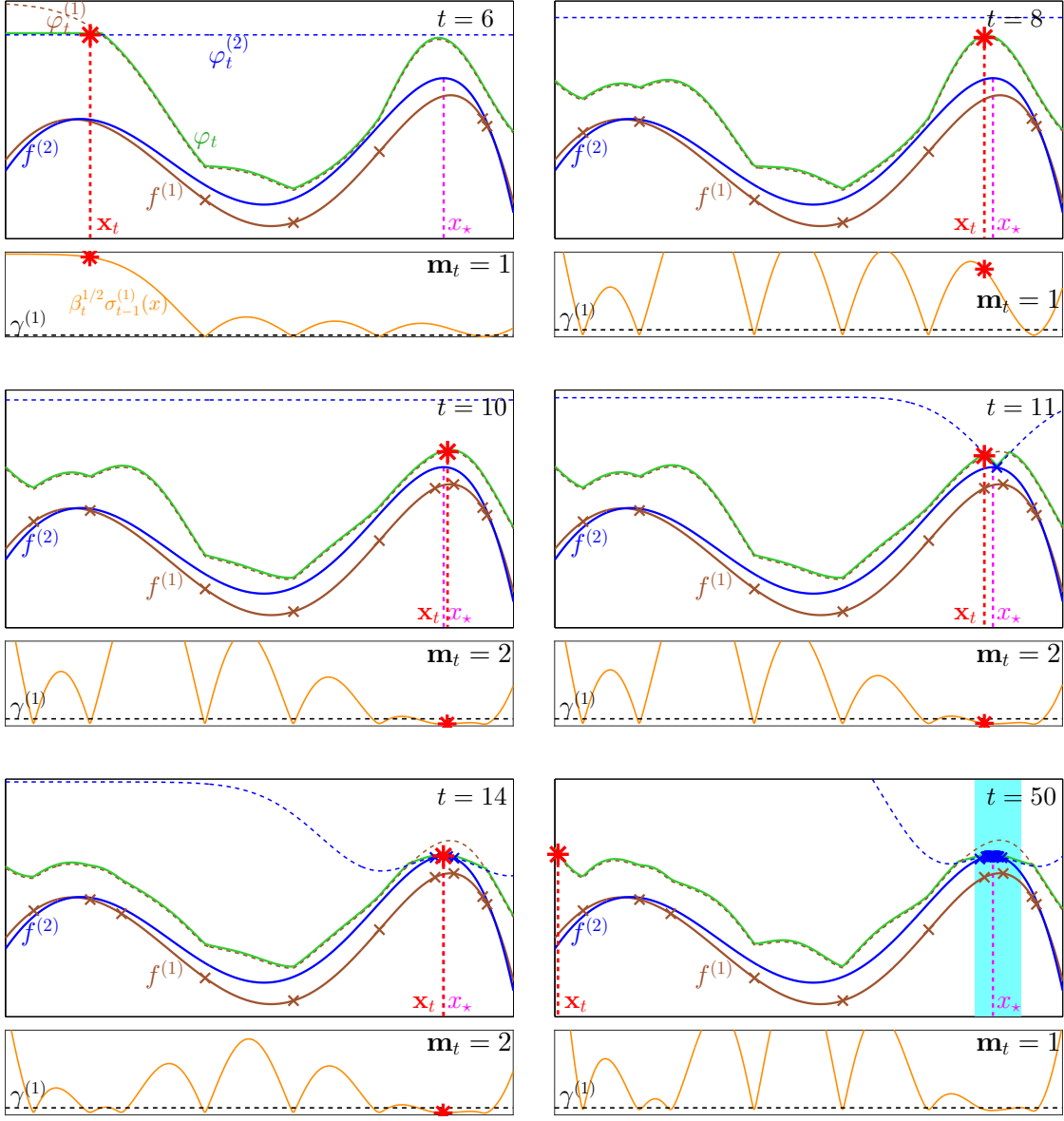


Figure 4: The 6 panels illustrate an execution of MF-GP-UCB in 2 fidelities at times $t = 6, 8, 10, 11, 14, 50$. In each panel, the top figure illustrates the upper bounds and selection of x_t while the bottom figure illustrates the selection of m_t . We have initialised MF-GP-UCB with 5 random points at the first fidelity. In the top figures, the solid lines in brown and blue are $f^{(1)}, f^{(2)}$ respectively, and the dashed lines are $\varphi_t^{(1)}, \varphi_t^{(2)}$. The solid green line is $\varphi_t = \min(\varphi_t^{(1)}, \varphi_t^{(2)})$. The small crosses are queries from 1 to $t - 1$ and the red star is the maximiser of φ_t , i.e. the next query x_t . x_* , the optimum of $f^{(2)}$ is shown in magenta. In the bottom figures, the solid orange line is $\beta_t^{1/2} \sigma_{t-1}^{(1)}$ and the dashed black line is $\gamma^{(1)}$. When $\beta_t^{1/2} \sigma_{t-1}^{(1)}(x_t) \leq \gamma^{(1)}$ we play at fidelity $m_t = 2$ and otherwise at $m_t = 1$. The cyan region in the last panel is the “good set” \mathcal{X}_g described in Section 5.1.

An Illustration of MF-GP-UCB: Figure 4 illustrates MF-GP-UCB via a simulation on a 2-fidelity problem. At the initial stages, MF-GP-UCB is mostly exploring \mathcal{X} in the first fidelity. $\beta_t^{1/2}\sigma_{t-1}^{(1)}$ is large and we are yet to constrain $f^{(1)}$ well to proceed to $m = 2$. At $t = 10$, we have constrained $f^{(1)}$ sufficiently well at a region around the optimum. $\beta_t^{1/2}\sigma_{t-1}^{(1)}(x_t)$ falls below $\gamma^{(1)}$ and we query at $m_t = 2$. Notice that once we do this (at $t = 11$), $\varphi_t^{(2)}$ dips to change φ_t in that region. At $t = 14$, MF-GP-UCB has identified the maximum x_* with just 4 queries to $f^{(2)}$. The region shaded in cyan in the last figure is the “good set” \mathcal{X}_g , which we alluded to in Section 2. We will define it formally and explain its significance in the multi-fidelity set up shortly. Our analysis predicts that most second fidelity queries in MF-GP-UCB will be confined to this set (roughly) and the simulation corroborates this claim. For example, in the last figure, at $t = 50$, the algorithm decides to explore at a point far away from the optimum. However, this query occurs in the first fidelity since we have not sufficiently constrained $f^{(1)}(x_t)$ in this region and $\beta_t^{1/2}\sigma_{t-1}^{(1)}(x_t)$ is large. The key idea is that it is *not necessary* to query such regions at the second fidelity as the first fidelity alone is enough to conclude that it is suboptimal. In addition, observe that in a large portion of \mathcal{X} , φ_t is given by $\varphi_t^{(1)}$ except in a small neighborhood around x_* , where it is given by $\varphi_t^{(2)}$.

Next we present our main theoretical results. We wish to remind the reader that a table of notations is available in Appendix B.2.

5. Theoretical Results

5.1 A Preview of our Theorems

We begin an informal yet intuitive introduction to our theorems in $M = 2$ fidelities. In this subsection, we will ignore constants and polylog terms when they are dominated by other terms. $\lesssim, \gtrsim, \asymp$ denote inequality and equality ignoring constants. When $A \subset \mathcal{X}$, we will denote its complement by \overline{A} .

Fundamental to the 2-fidelity problem is the good set $\mathcal{X}_g = \{x \in \mathcal{X}; f_* - f^{(1)}(x) \leq \zeta^{(1)}\}$. \mathcal{X}_g is a high-valued region for $f^{(2)}(x)$: for all $x \in \mathcal{X}_g$, $f^{(2)}(x)$ is at most $2\zeta^{(1)}$ away from the optimum. If a multi-fidelity strategy were to use *all* its second fidelity queries only in \mathcal{X}_g , then the regret will only have $\Psi_n(\mathcal{X}_g)$ dependence after n high fidelity queries. In contrast, a strategy that only operates at the highest fidelity (e.g. GP-UCB) will have $\Psi_n(\mathcal{X})$ dependence. When $\zeta^{(1)}$ is small, i.e. when $f^{(1)}$ is a good approximation to $f^{(2)}$, \mathcal{X}_g will be much smaller than \mathcal{X} . Then, $\Psi_n(\mathcal{X}_g) \ll \Psi_n(\mathcal{X})$, and the multi-fidelity strategy will have significantly better regret than a single fidelity strategy. Alas, achieving this somewhat ideal goal is not possible without perfect knowledge of the approximation. However, with MF-GP-UCB we can come quite close. We can show that *most* second fidelity queries are confined to the slightly inflated good set $\mathcal{X}_{g,\rho} = \{x \in \mathcal{X}; f_* - f^{(1)}(x) \leq \zeta^{(1)} + \rho\gamma^{(1)}\}$. Here $\rho > 0$ is a parameter which will be explained in our theorems. The following lemma bounds the number of first and second fidelity evaluations in $\mathcal{X}_{g,\rho}$ and its complement $\overline{\mathcal{X}_{g,\rho}}$. We denote the number of queries at the m^{th} fidelity in a set $A \subset \mathcal{X}$ within the first n time steps by $T_n^{(m)}(A)$.

Lemma 4 (Informal, Bounding the number of evaluations for $M = 2$) *Let $\mathcal{X} \subset [0, r]^d$. Consider MF-GP-UCB after n total evaluations at either fidelity. Then, for all $\alpha \in (0, 1)$, there exists $\rho > 0$ depending only on α such that the following statements hold with high probability,*

$$T_n^{(1)}(\overline{\mathcal{X}_{g,\rho}}) \lesssim \text{sublinear}(n) \cdot \Pi(\mathcal{X}_{g,\rho}), \quad T_n^{(1)}(\mathcal{X}_{g,\rho}) \lesssim \frac{\text{polylog}(n)}{\gamma^{(1)^2}} \cdot \Pi(\mathcal{X}_{g,\rho}),$$

$$T_n^{(2)}(\overline{\mathcal{X}_{g,\rho}}) \lesssim n^\alpha \cdot \Pi(\overline{\mathcal{X}_{g,\rho}}), \quad T_n^{(2)}(\mathcal{X}_{g,\rho}) \asymp n.$$

Here $\Pi(A)$ scales with the size of A ; it is $|A|$ for discrete A and $\text{vol}(A)$ for continuous A . The sublinear(n) term for $T_n^{(1)}$ is $\text{polylog}(n)$ for discrete \mathcal{X} and $\text{poly}(n)$ for continuous compact \mathcal{X} .

The above lemma will be useful for two reasons. First, the bounds on $T_n^{(2)}(\cdot)$ show that most second fidelity (expensive) queries are inside $\mathcal{X}_{g,\rho}$. The number of second fidelity (expensive) queries outside $\mathcal{X}_{g,\rho}$ is small, precisely $\asymp n^\alpha$ for all $\alpha > 0$ for an appropriate ρ . This *strong* result is only possible in the multi-fidelity setting. In GP-UCB the best achievable bound on the number of plays on a suboptimal set is $\asymp n^{1/2}$ for the SE kernel and worse for the Matérn kernel. For example, in the simulation of Figure 4, all queries to $f^{(2)}$ are in fact confined to \mathcal{X}_g which is a subset of $\mathcal{X}_{g,\rho}$. This allows us to obtain regret that scales with $\Psi_n(\mathcal{X}_{g,\rho})$ as explained above. Second, we will use Lemma 4 to control N , the (random) number of queries by MF-GP-UCB within capital Λ . Let $n_\Lambda = \lfloor \Lambda/\lambda^{(2)} \rfloor$ be the (non-random) number of queries by a single fidelity method operating only at the second fidelity. As $\lambda^{(1)} < \lambda^{(2)}$, N could be large for an arbitrary multi-fidelity method. However, using the bounds on $T_n^{(1)}(\cdot)$ we can show that N is $\asymp n_\Lambda$ when Λ is larger than some value Λ_0 . Below, we detail the main ingredients in the proof of Lemma 4.

- $T_n^{(1)}(\overline{\mathcal{X}_{g,\rho}})$: By the design of our algorithm, MF-GP-UCB will begin querying $f^{(1)}$. To achieve finite regret we need to show that we will eventually query $f^{(2)}$. For any region in $\mathcal{X}_{g,\rho}$ the switching condition of step 2 in Algorithm 2 ensures that we do not query that region indefinitely. That is, if we keep querying a certain region, the first fidelity GP uncertainty $\beta_t^{1/2} \sigma_{t-1}^{(m)}$ will reduce below $\gamma^{(1)}$ in that region. As expected, the bound has critical dependence on the threshold parameter $\gamma^{(1)}$. We will discuss the implications at the end of this subsection and in Section 6.
- $T_n^{(1)}(\mathcal{X}_{g,\rho})$: For queries to $f^{(1)}$ outside $\mathcal{X}_{g,\rho}$, we obtain a tighter, $\gamma^{(1)}$ independent, bound using a simple argument. As $f^{(1)}$ is small outside $\mathcal{X}_{g,\rho}$, it is unlikely to contain the UCB maximiser and be selected in step 1 of Algorithm 2 several times.
- $T_n^{(2)}(\overline{\mathcal{X}_{g,\rho}})$: We appeal to previous first fidelity queries. If we are querying at the second fidelity at a certain region, it can only be because the first fidelity confidence band is small. This implies that there must be several first fidelity queries in that region which in turn implies that we can learn about $f^{(1)}$ with high confidence. As $f^{(1)}$ alone would tell us that any point in $\mathcal{X}_{g,\rho}$ is suboptimal for $f^{(2)}$, the maximiser of the UCB is unlikely to lie in this region frequently. Hence, we will not query outside $\mathcal{X}_{g,\rho}$ often. The threshold parameter $\gamma^{(1)}$ does appear in the bound, but its dependence is very mild.

It follows from the above that the number of second fidelity queries in $\mathcal{X}_{g,\rho}$ scales $T_n^{(2)}(\mathcal{X}_{g,\rho}) \asymp n$. Finally, we invoke techniques from Srinivas et al. (2010) to control the regret using the MIG. However, unlike them, we analyse the MIG of $\mathcal{X}_{g,\rho}$ and $\overline{\mathcal{X}_{g,\rho}}$ separately as the number of second fidelity queries are different for each subset. This allows us to obtain a tighter bound on $R(\Lambda)$ of the following form.

Theorem 5 (Informal, Regret of MF-GP-UCB for $M = 2$) *Let $\mathcal{X} \subset [0, r]^d$. Then, for all $\alpha \in (0, 1)$, there exists $\rho > 0$, Λ_0 such that for all $\Lambda > \Lambda_0$ the following holds with high probability.*

$$S(\Lambda) \lesssim \sqrt{\frac{\beta_{n_\Lambda} \Psi_{n_\Lambda}(\mathcal{X}_{g,\rho})}{n_\Lambda}} + \sqrt{\frac{\beta_{n_\Lambda} \Psi_{n_\Lambda}^\alpha(\mathcal{X})}{n_\Lambda^{2-\alpha}}}$$

Here ρ depends only on α and Λ_0 depends on α , $\gamma^{(1)}$, $\lambda^{(1)}$ and the approximation $f^{(1)}$.

It is instructive to compare the above rates against that for GP-UCB in Theorem 3. By dropping the common and sub-dominant terms, the rate for GP-UCB is $\Psi_{n_\Lambda}^{1/2}(\mathcal{X})$ whereas for MF-GP-UCB it is $\Psi_{n_\Lambda}^{1/2}(\mathcal{X}_{g,\rho}) + n_\Lambda^{\alpha-1}\Psi_{n_\Lambda}^{1/2}(\mathcal{X})$. The latter term for MF-GP-UCB is small due to the decaying $n_\Lambda^{\alpha-1}$ term and since the MIG's dependence scales as n_Λ^α . Therefore, the first term dominates and whenever the approximation is very good ($\text{vol}(\mathcal{X}_{g,\rho}) \ll \text{vol}(\mathcal{X})$) the rates for MF-GP-UCB are very appealing. When the approximation worsens and $\mathcal{X}_g, \mathcal{X}_{g,\rho}$ become larger, the bound decays gracefully. In the worst case, MF-GP-UCB is never worse than GP-UCB up to constant terms for $\Lambda \geq \Lambda_0$. The Λ_0 term is required since at the initial stages, MF-GP-UCB will be exploring $f^{(1)}$ before proceeding to $f^{(2)}$, at which stage its regret will still be $+\infty$. The costs $\lambda^{(1)}, \lambda^{(2)}$ get factored into the result via the $\Lambda > \Lambda_0$ condition. If $\lambda^{(1)}$ is large, for fixed $\gamma^{(1)}$, a larger amount of capital is spent at the first fidelity, so Λ_0 will be large.

Now let us analyse the effect of the parameter $\gamma^{(1)}$ on the result. At first sight, large $\gamma^{(1)}$ seems to increase the size of $\mathcal{X}_{g,\rho}$ which would suggest that we should keep it as small as possible. However, smaller $\gamma^{(1)}$ also increases Λ_0 ; intuitively, if $\gamma^{(1)}$ is too small, then one will wait for a long time in step 2 of Algorithm 2 for $\beta_t^{1/2}\sigma_{t-1}^{(1)}$ to decrease without proceeding to $f^{(2)}$. As one might expect, an optimal choice of $\gamma^{(1)}$ depends on $\lambda^{(1)}$; for e.g. if the approximation is extremely cheap, it makes sense to use very small $\gamma^{(1)}$ and learn as much as possible about $f^{(2)}$ from $f^{(1)}$. However, it also depends on other problem dependent quantities such as \mathcal{X}_g . In Kandasamy et al. (2016a) we were able to exactly specify a practical choice for $\gamma^{(1)}$ in the K -armed setting, which, unfortunately is not as straightforward in the GP setting. In Section 6 we describe a heuristic to set the $\gamma^{(m)}$ values which worked well in our experiments.

For general M , we will define a hierarchy of “good sets”, the complement of which will be eliminated when we proceed from one fidelity to the next. At the highest fidelity, we will be querying mostly inside a small subset of \mathcal{X} informed by the approximations $f^{(1)}, \dots, f^{(M-1)}$. We will formalise these intuitions in the next two subsections.

5.2 Discrete \mathcal{X}

We first analyse when \mathcal{X} is a discrete subset of $[0, r]^d$. Denote $\Delta^{(m)}(x) = f_\star - f^{(m)}(x) - \zeta^{(m)}$ and $\mathcal{J}_\eta^{(m)} = \{x \in \mathcal{X}; \Delta^{(m)}(x) \leq \eta\}$. Let $\rho > 1$ be given. Central to our analysis will be the partitioning $(\mathcal{H}^{(m)})_{m=1}^M$ of \mathcal{X} . First define $\mathcal{H}^{(1)} = \overline{\mathcal{J}}_{\rho\gamma}^{(1)} = \{x : f^{(1)}(x) < f_\star - \zeta^{(1)} - \rho\gamma^{(1)}\}$ to be the arms whose $f^{(1)}$ value is at least $\zeta^{(1)} + \rho\gamma^{(1)}$ below the optimum f_\star . Then recursively define,

$$\mathcal{H}^{(m)} = \overline{\mathcal{J}}_{\rho\gamma}^{(m)} \cap \left(\bigcap_{\ell=1}^{m-1} \mathcal{J}_{\rho\gamma}^{(\ell)} \right) \quad \text{for } 2 \leq m \leq M-1, \quad \mathcal{H}^{(M)} = \bigcap_{\ell=1}^{M-1} \mathcal{J}_{\rho\gamma}^{(\ell)}. \quad (5)$$

In addition to the above, we will also find it useful to define the sets “above” $\mathcal{H}^{(m)}$ as $\widehat{\mathcal{H}}^{(m)} = \bigcup_{\ell=m+1}^M \mathcal{H}^{(\ell)}$ and the sets “below” $\mathcal{H}^{(m)}$ as $\check{\mathcal{H}}^{(m)} = \bigcup_{\ell=1}^{m-1} \mathcal{H}^{(\ell)}$. Our analysis reveals that most of the capital invested at points in $\mathcal{H}^{(m)}$ will be due to queries to the m^{th} fidelity function $f^{(m)}$. $\check{\mathcal{H}}^{(m)}$ is the set of points that can be excluded from queries at fidelities m and beyond due to information from lower fidelities. $\widehat{\mathcal{H}}^{(m)}$ are points that will be queried at fidelities higher than m several times. In the 2 fidelity setting described in Section 5, $\mathcal{X}_{g,\rho} = \mathcal{H}^{(2)}$ and $\overline{\mathcal{X}}_{g,\rho} = \mathcal{H}^{(1)} = \check{\mathcal{H}}^{(2)}$. We have illustrated these sets in Figure 5. We now state our main theorem for the discrete case.

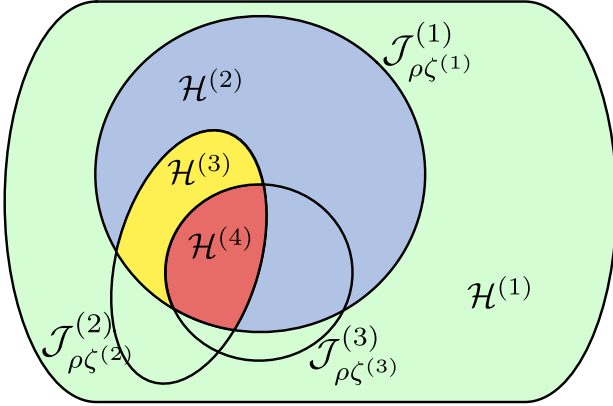


Figure 5: Illustration of the partition $\mathcal{H}^{(m)}$'s for a $M = 4$ fidelity problem. The sets $\mathcal{J}_0^{(m)}$ are indicated next to their boundaries. The sets $\mathcal{H}^{(1)}, \mathcal{H}^{(2)}, \mathcal{H}^{(3)}, \mathcal{H}^{(4)}$ are shown in green, blue, yellow and red respectively. Most of the capital invested at points in $\mathcal{H}^{(m)}$ will be due to queries to the m^{th} fidelity function $f^{(m)}$.

Theorem 6 Let \mathcal{X} be a discrete subset of $[0, r]^d$. Let $f^{(m)} \sim \mathcal{GP}(\mathbf{0}, \kappa)$ for all m . Assume that $f^{(m)}$'s satisfy assumptions **A1**, **A2** and κ satisfies Assumption 2. Pick $\delta \in (0, 1)$ and run MF-GP-UCB with $\beta_t = 2 \log(M|\mathcal{X}|\pi^2 t^2 / (3\delta))$. Then, for all $\alpha \in (0, 1)$, there exists ρ, Λ_0 such that, with probability $> 1 - \delta$ we have for all $\Lambda \geq \Lambda_0$,

$$S(\Lambda) \leq \sqrt{\frac{2C_1 \beta_{2n_\Lambda} \Psi_{2n_\Lambda}(\mathcal{H}^{(M)})}{n_\Lambda}} + \sqrt{\frac{2C_1 |\mathcal{X}| \beta_{2n_\Lambda} \Psi_{2n_\Lambda}^\alpha(\mathcal{X})}{n_\Lambda^{2-\alpha}}}.$$

Here $C_1 = 8 / \log(1 + \eta^2)$ is a constant and $n_\Lambda = \lfloor \Lambda / \lambda^{(M)} \rfloor$ is the number of queries by an algorithm which ignores the lower fidelities. $\rho = \max(2, 1 + \sqrt{1/2 + 1/\alpha})$ depends only on α . Λ_0 depends on several problem dependent quantities including the sizes of the sets $\mathcal{H}^{(m)}$ and consequently on ρ .

First note that $\Psi_n(\cdot) \asymp \Psi_{2n}(\cdot)$ and that $\beta_n \asymp \beta_{2n} \asymp \log(n)$. When comparing to the result in Theorem 3, we see that we outperform GP-UCB by a factor of $\sqrt{\Psi_{n_\Lambda}(\mathcal{H}^{(M)}) / \Psi_{n_\Lambda}(\mathcal{X})}$ asymptotically. The set $\mathcal{H}^{(M)}$ from (5) is determined by the $\zeta^{(1)}, \dots, \zeta^{(M-1)}$ values, the approximations $f^{(1)}, \dots, f^{(M-1)}$ and the parameters $\gamma^{(1)}, \dots, \gamma^{(M-1)}$. The better the approximations, the smaller the set $\mathcal{H}^{(M)}$ and there is more advantage over single fidelity strategies. As the approximations worsen, the advantage to multi-fidelity optimisation diminishes as expected, but we are never worse than GP-UCB up to constant factors.

5.3 Continuous and Compact \mathcal{X}

As for discrete \mathcal{X} we will begin with a partitioning of \mathcal{X} . The partitioning will depend on the $\gamma^{(m)}$ values as before, but in addition will also depend on a parameter $\tau > 0$. Let $\mathcal{J}_\eta^{(m)} = \{x \in \mathcal{X}; \Delta^{(m)}(x) \leq \eta\}$ be as defined in the discrete case. We make the dependence on τ explicit and define $\mathcal{H}_\tau^{(1)} = \overline{\mathcal{J}}_{\max(\tau, \rho\gamma)}^{(1)} = \{x : f^{(1)}(x) < f_\star - \zeta^{(1)} - \max(\tau, \rho\gamma^{(1)})\}$ to be the subset whose $f^{(1)}$ value is at least $\zeta^{(1)} + \max(\tau, \rho\gamma^{(1)})$ below the optimum f_\star . Then define,

$$\mathcal{H}_\tau^{(m)} = \overline{\mathcal{J}}_{\max(\tau, \rho\gamma)}^{(m)} \cap \left(\bigcap_{\ell=1}^{m-1} \mathcal{J}_{\max(\tau, \rho\gamma)}^{(\ell)} \right) \text{ for } 2 \leq m \leq M-1, \quad \mathcal{H}_\tau^{(M)} = \bigcap_{\ell=1}^{M-1} \mathcal{J}_{\max(\tau, \rho\gamma)}^{(\ell)}. \quad (6)$$

The purpose of τ is to create a ‘‘separation’’ between the function values in the sets. In the discrete case, this separation is guaranteed as the function values $f^{(m)}(x)$ is a discrete set. This however, is

not the case in continuous settings. The requirement $\tau > 0$ is mostly a technical condition and is otherwise orthogonal to the gist of our theorems. Indeed, our theorems hold for all $\tau > 0$.

Finally, for any given $\alpha > 0$ we will also define

$$\mathcal{H}_{\tau,n}^{(m)} = \left\{ x \in \mathcal{X} : B_2(x, r\sqrt{d}/n^{\frac{\alpha}{2d}}) \cap \mathcal{H}_{\tau}^{(m)} \neq \emptyset \quad \wedge \quad x \notin \widehat{\mathcal{H}}^{(m)} \right\}$$

to be an n -dependent L_2 dilation of $\mathcal{H}_{\tau,n}^{(m)}$ by $r\sqrt{d}/n^{\frac{\alpha}{2d}}$. Here, $B_2(x, \epsilon)$ is an L_2 ball of radius ϵ centred at x . The sets $\{\mathcal{H}_{\tau,n}^{(m)}\}_{m=1}^M$ depend on ρ, γ, τ, n and α . Notice that for any $\alpha > 0$, as $n \rightarrow \infty$, $\mathcal{H}_{\tau,n}^{(m)} \rightarrow \mathcal{H}_{\tau}^{(m)}$. Our main theorem is as follows.

Theorem 7 *Let $\mathcal{X} \subset [0, r]^d$ be compact and convex. Let $f^{(m)} \sim \mathcal{GP}(\mathbf{0}, \kappa) \forall m$, and satisfy assumptions **A2**, **A3**. Let κ satisfy Assumption 2 with some constants a, b . Pick $\delta \in (0, 1)$ and run MF-GP-UCB with*

$$\beta_t = 2 \log \left(\frac{M\pi^2 t^2}{2\delta} \right) + 4d \log(t) + \max \left\{ 0, 2d \log \left(brd \log \left(\frac{6Mad}{\delta} \right) \right) \right\}.$$

Then, for all $\alpha \in (0, 1)$ and $\tau > 0$, there exists ρ, Λ_0 such that with probability at least $1 - \delta$ we have for all $\Lambda \geq \Lambda_0$,

$$S(\Lambda) \leq \sqrt{\frac{2C_1 \beta_{2n_\Lambda} \Psi_{2n_\Lambda}(\mathcal{H}_{\tau, n_\Lambda}^{(M)})}{n_\Lambda}} + \sqrt{\frac{2C_1 M \beta_{2n_\Lambda} \Psi_{2Mn_\Lambda}(\mathcal{X})}{n_\Lambda^{2-\alpha}}} + \frac{\pi^2}{6n_\Lambda}.$$

Here $C_1 = 8/\log(1 + \eta^2)$ is a constant and $n_\Lambda = \lfloor \Lambda/\lambda^{(M)} \rfloor$ is the number of queries by an algorithm which ignores the lower fidelities. ρ depends only on α and satisfies $\rho > \rho_0 = \max\{2, 1 + \sqrt{(1 + 2/\alpha)/(1 + d)}\}$. Λ_0 depends on several problem dependent quantities including the volumes of the sets $\mathcal{H}_{\tau}^{(m)}$ and consequently on ρ .

The comparison of the above bound against GP-UCB is similar to the discrete case. The main difference is that we have an additional dilation of $\mathcal{H}_{\tau}^{(M)}$ to $\mathcal{H}_{\tau, n_\Lambda}^{(M)}$ which occurs due to a covering argument in our analysis. Recall that $\mathcal{H}_{\tau, n_\Lambda}^{(m)} \rightarrow \mathcal{H}_{\tau}^{(M)}$ as $\Lambda \rightarrow \infty$. The bound is determined by the MIG of the set $\mathcal{H}_{\tau, n_\Lambda}^{(M)}$, which is small when the approximations are good.

6. Some Implementation Details of MF-GP-UCB and other Baselines

Our implementation uses some standard techniques in the Bayesian optimisation literature given below. In addition, we describe the heuristics used to set the $\gamma^{(m)}, \zeta^{(m)}$ parameters of our method.

Initialisation and Kernel: Following recommendations in Brochu et al. (2010) all GP methods were initialised with uniform random queries using an initialisation capital Λ_0 . For single fidelity methods, we used it at the M^{th} fidelity, whereas for multi-fidelity methods we used $\Lambda_0/2$ at the first fidelity and $\Lambda_0/2$ at the second fidelity. Next, we initialise the kernel by maximising the GP marginal likelihood (Rasmussen and Williams, 2006). We update the kernel every 25 iterations again using marginal likelihood.

Choice of β_t : β_t , as specified in Theorems 3, 7 has unknown constants and tends to be too conservative in practice. Following Kandasamy et al. (2015) we use $\beta_t = 0.2d \log(2t)$ which captures the dominant dependencies on d and t .

Maximising φ_t : We used the DiRect algorithm (Jones et al., 1993).

Choice of $\zeta^{(m)}$'s: Algorithm 2 assumes that the $\zeta^{(m)}$'s are given with the problem description, which is hardly the case in practice. In our implementation, instead of having to deal with $M - 1$, $\zeta^{(m)}$ values we will assume $\|f^{(m)} - f^{(m-1)}\|_\infty \leq \zeta$. This satisfies assumption **A2** with $(\zeta^{(1)}, \zeta^{(2)}, \dots, \zeta^{(M-1)}) = ((M - 1)\zeta, (M - 2)\zeta, \dots, \zeta)$. This allows us to work with only one value of ζ . We initialise ζ to a small value, 1% of the range of initial queries. Whenever we query at any fidelity $m > 1$ we also check the posterior mean of the $(m - 1)^{\text{th}}$ fidelity. If $|f^{(m)}(x_t) - \mu_{t-1}^{(m-1)}(x_t)| > \zeta$, we query again at x_t , but at the $(m - 1)^{\text{th}}$ fidelity. If $|f^{(m)}(x_t) - f^{(m-1)}(x_t)| > \zeta$, we update ζ to twice the violation.

Choice of $\gamma^{(m)}$'s: For this, we use the following intuition: if the algorithm, is stuck at fidelity m for too long, then $\gamma^{(m)}$ is probably too small. We start with small values for all $\gamma^{(m)}$. If the algorithm does not query above the m^{th} fidelity for more than $\lambda^{(m+1)}/\lambda^{(m)}$ iterations, we double $\gamma^{(m)}$. All $\gamma^{(m)}$ values were initialised to 1% of the range of initial queries.

We found our implementation to be fairly robust even recovering from fairly bad approximations at the lower fidelities (see Appendix A.3).

7. Experiments

We present experiments for compact and continuous \mathcal{X} since it is the more practically relevant setting. We compare MF-GP-UCB to the following baselines. **Single fidelity methods:** GP-UCB; El: the expected improvement criterion for BO (Jones et al., 1998); DiRect: the dividing rectangles method (Jones et al., 1993). **Multi-fidelity methods:** MF-NAIVE: a naive baseline where we use GP-UCB to query at the *first* fidelity a large number of times and then query at the last fidelity at the points queried at $f^{(1)}$ in decreasing order of $f^{(1)}$ -value; MF-SKO: the multi-fidelity sequential kriging method from (Huang et al., 2006). Previous works on multi-fidelity methods (including MF-SKO) had not made their code available and were not straightforward to implement. Hence, we could not compare to all of them. We discuss this more in Appendix A.1 along with some other single and multi-fidelity baselines we tried but excluded in the comparison to avoid clutter in the figures. We also detail some design choices and hyper-parameters for the baselines in Appendix A.1.

7.1 Synthetic Examples

We use the Currin exponential ($d = 2$), Park ($d = 4$) and Borehole ($d = 8$) functions in $M = 2$ fidelity experiments and the Hartmann functions in $d = 3$ and 6 with $M = 3$ and 4 fidelities respectively. The first three functions are taken from previous multi-fidelity literature (Xiong et al., 2013) while we tweaked the Hartmann functions to obtain the lower fidelities for the latter two cases. In Appendix A we give the formulae for these functions and the approximations used for the lower fidelities. We show the simple regret $S(\Lambda)$ against capital Λ in Figure 6. MF-GP-UCB outperforms other baselines on all problems.

The last panel of Figure 6 shows a histogram of the number of queries at each fidelity after 184 queries of MF-GP-UCB, for different ranges of $f^{(3)}(x)$ for the Hartmann-3D function. Many of the queries at the low $f^{(3)}$ values are at fidelity 1, but as we progress they decrease and the second fidelity queries increase. The third fidelity dominates very close to the optimum but is used sparingly

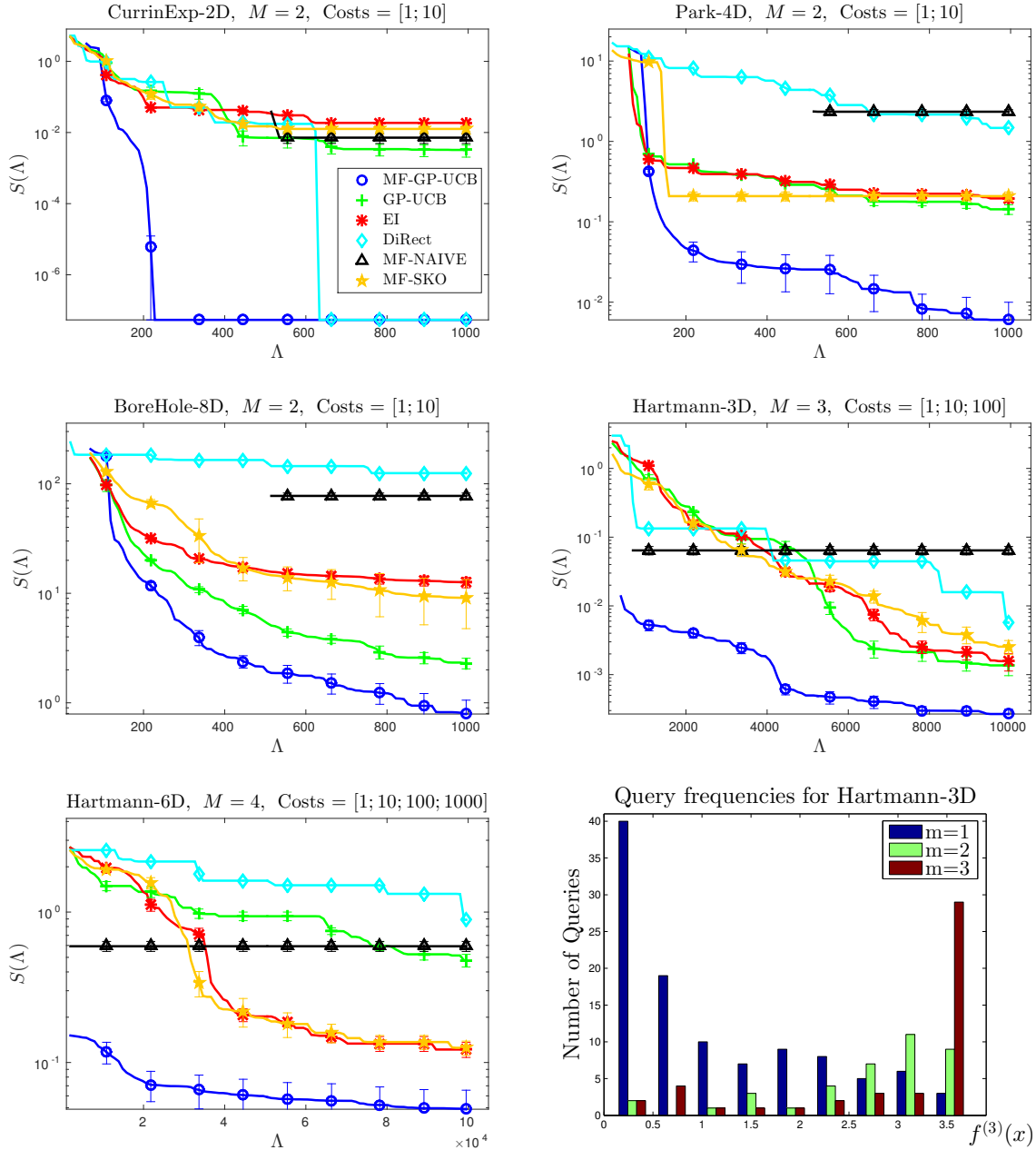


Figure 6: The simple regret $S(\Lambda)$ (3) against the spent capital Λ on the synthetic functions. The title states the function, its dimensionality, the number of fidelities and the costs we used for each fidelity in the experiment. All curves barring DiRect (which is a deterministic), were produced by averaging over 20 experiments. The error bars indicate one standard error. All figures follow the legend in the first figure for the Currin exponential function. The last panel shows the number of queries at different function values at each fidelity for the Hartmann-3D example.

elsewhere. This corroborates the prediction in our analysis that MF-GP-UCB uses low fidelities to explore and successively higher fidelities at promising regions to zero in on x_* . (Also see Figure 4.)

A common occurrence with MF-NAIVE was that once we started querying at fidelity M , the regret barely decreased. The diagnosis in all cases was the same: it was stuck around the maximum of $f^{(1)}$ which is suboptimal for $f^{(M)}$. This suggests that while we have cheap approximations, the problem is by no means trivial. As explained previously, it is also important to “explore” at higher fidelities to achieve good regret. The efficacy of MF-GP-UCB when compared to single fidelity methods is that it confines this exploration to a small set containing the optimum.

In our experiments we found that MF-SKO did not consistently beat other single fidelity methods. Despite our best efforts to reproduce this method, we found it to be quite brittle. In fact, we also tried another multi-fidelity method and found that it did not perform as desired (See Appendix A.1 for more details). In Appendix A.3 we present additional experiments to test our implementation of MF-GP-UCB. We study how it performs under bad approximations and when the cost of the approximation varies.

7.2 Real Experiments

We present results on three hyper-parameter tuning tasks and a maximum likelihood inference task in Astrophysics. We compare methods on computation time since that is the “cost” in all experiments. We include the processing time for each method in the comparison (i.e. the cost of determining the next query). The results are given in Figure 7 where MF-GP-UCB outperforms other baselines on all tasks. The experimental set up for each optimisation problem is described below.

Classification using SVMs (SVM): We trained a Support vector classifier on the magic gamma dataset using the sequential minimal optimisation algorithm to an accuracy of 10^{-12} . The goal is to tune the kernel bandwidth and the soft margin coefficient in the ranges $(10^{-3}, 10^1)$ and $(10^{-1}, 10^5)$ respectively on a dataset of size 2000. We set this up as a $M = 2$ fidelity experiment with the entire training set at the second fidelity and 500 points at the first. Each query to $f^{(m)}$ required 5-fold cross validation on the respective training sets.

Regression using additive kernels (SALSA): We used the SALSA method for additive kernel ridge regression (Kandasamy and Yu, 2016) on the 4-dimensional coal power plant dataset. We tuned the 6 hyper-parameters –the regularisation penalty, the kernel scale and the kernel bandwidth for each dimension– each in the range $(10^{-3}, 10^4)$ using 5-fold cross validation. This experiment used $M = 3$ and 2000, 4000, 8000 points at each fidelity respectively.

Viola & Jones face detection (V&J): The Viola & Jones cascade face classifier (Viola and Jones, 2001), which uses a cascade of weak classifiers, is a popular method for face detection. To classify an image, we pass it through each classifier. If at any point the classifier score falls below a threshold, the image is classified as negative. If it passes through the cascade, then it is classified as positive. One of the more popular implementations comes with OpenCV and uses a cascade of 22 weak classifiers. The threshold values in the OpenCV implementation are pre-set based on some heuristics and there is no reason to think they are optimal for a given face detection problem. The goal is to tune these 22 thresholds by optimising them over a training set. We modified the OpenCV implementation to take in the thresholds as parameters. As our domain \mathcal{X} we chose a neighbourhood around the configuration used in OpenCV. We set this up as an $M = 2$ fidelity experiment where the second fidelity used 3000 images from the Viola and Jones face database and the first used just

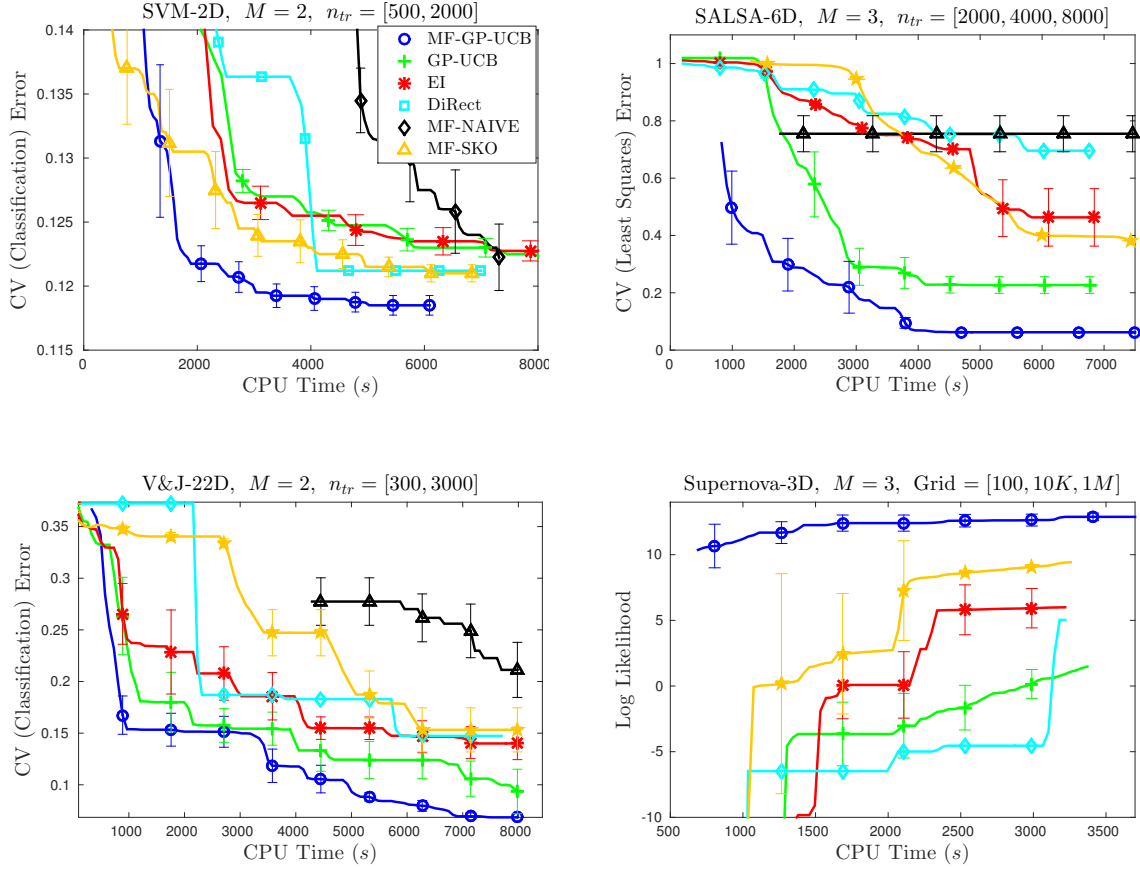


Figure 7: Results on the real experiments. The first three figures are hyper-parameter tuning tasks while the last is an astrophysical maximum likelihood problem. The title states the experiment, dimensionality (number of hyper-parameters or cosmological parameters) and the number of fidelities. For the three hyper-parameter tuning tasks we plot the best cross validation error (lower is better) and for the astrophysics task we plot the highest log likelihood (higher is better). For the hyper-parameter tuning tasks we obtained the lower fidelities by using smaller training sets, indicated by n_{tr} in the figures and for the astrophysical problem we used a coarser grid for numerical integration, indicated by “Grid”. MF-NAIVE is not visible in the last experiment because it performed very poorly. All curves were produced by averaging over 10 experiments. The error bars indicate one standard error. The lengths of the curves are different in time as we ran each method for a pre-specified number of iterations and they concluded at different times.

300. Interestingly, on an independent test set, the configurations found by MF-GP-UCB consistently achieved over 90% accuracy while the OpenCV configuration achieved only 87.4% accuracy.

Type Ia Supernovae (Supernova): We use Type Ia supernovae data from [Davis et al \(2007\)](#) for maximum likelihood inference on 3 cosmological parameters, the Hubble constant $H_0 \in (60, 80)$, the dark matter fraction $\Omega_M \in (0, 1)$ and the dark energy fraction $\Omega_\Lambda \in (0, 1)$. Unlike typical parametric maximum likelihood problems we see in machine learning, the likelihood is only available as a black-box. It is computed using the Robertson–Walker metric which requires a (one dimensional) numerical integration for each sample in the dataset. We set this up as a $M = 3$ fidelity task. At the third fidelity, the integration was performed using the trapezoidal rule on a grid of size 10^6 . For the first and second fidelities, we used grids of size $10^2, 10^4$ respectively. The goal is to maximise the likelihood at the third fidelity.

8. Proofs

In this section we present the proofs of our main theorems. While it is self contained, the reader will benefit from first reading the more intuitive discussion in Section 5. The goal in this section is to bound the simple regret $S(\Lambda)$ given in (3). Recall that N is the random number of plays within capital Λ . While $N \leq \lfloor \Lambda/\lambda^{(1)} \rfloor$ is a trivial upper bound for N , this will be too loose for our purposes. In fact, we will show that after a sufficiently large number of queries at any fidelity, the number of queries at fidelities smaller than M will be sublinear in N . Hence $N \in \mathcal{O}(n_\Lambda)$ where $n_\Lambda = \lfloor \Lambda/\lambda^{(M)} \rfloor$ is the number of plays by any algorithm that operates only at the highest fidelity.

We introduce some notation to keep track of the evaluations at each fidelity in MF-GP-UCB. After n steps, we will have queried multiple times at any of the M fidelities. $T_n^{(m)}(x)$ denotes the number of queries at $x \in \mathcal{X}$ at fidelity m after n steps. $T_n^{(m)}(A)$ denotes the same for a subset $A \subset \mathcal{X}$. $\mathcal{D}_n^{(m)} = \{(x_t, y_t)\}_{t:m_t=m}$ is the set of query-value pairs at the m^{th} fidelity until time n .

Roadmap: To bound $S(\Lambda)$ in both the discrete and continuous settings, we will begin by studying the algorithm after n evaluations at any fidelity and analyse the following quantity,

$$\tilde{R}_n = \sum_{\substack{t=1 \\ t:m_t=M}}^n f_\star - f^{(M)}(x_t). \quad (7)$$

Readers familiar with the bandit literature will see that this is similar to the notion of *cumulative regret*, except we only consider queries at the M^{th} fidelity. we will identify a set $\mathcal{Z} \subset \mathcal{X}$ which contains x_\star and has high value for the payoff function $f^{(M)}(x)$. \mathcal{Z} will be determined by the approximations provided via the lower fidelity evaluations. Then, we decompose \tilde{R}_n as follows,

$$\tilde{R}_n = \underbrace{\sum_{\substack{t:m_t=M \\ x_t \in \mathcal{Z}}} (f_\star - f^{(M)}(x_t))}_{\tilde{R}_{n,1}} + \underbrace{\sum_{\substack{t:m_t=M \\ x_t \in \bar{\mathcal{Z}}}} (f_\star - f^{(M)}(x_t))}_{\tilde{R}_{n,2}}. \quad (8)$$

$\tilde{R}_{n,1}$ is the cumulative regret at the M^{th} fidelity due to queries in \mathcal{Z} and $\tilde{R}_{n,2}$ is due queries outside \mathcal{Z} . We will bound $\tilde{R}_{n,1}, \tilde{R}_{n,2}$ separately using the MIGs (Definition 1) of \mathcal{Z} and $\bar{\mathcal{Z}}$; for this, we will use the techniques in [Srinivas et al. \(2010\)](#). However, we will show that $\tilde{R}_{n,1}$ dominates $\tilde{R}_{n,2}$

because most of the evaluations will be inside \mathcal{Z} in the multi-fidelity setting. Hence, the regret for MF-GP-UCB will scale with $\Psi_n(\mathcal{Z})$ instead of $\Psi_n(\mathcal{X})$ as is the case for GP-UCB. Finally, to convert this bound in terms of n to one that depends on Λ , we show that both the total number of evaluations N and the number of highest fidelity evaluations $T_N^{(M)}(\mathcal{X})$ are on the order of n_Λ when Λ_0 is sufficiently large. For this, we use the list of ingredients set out under Lemma 4 in Section 5.1. Then $S(\Lambda)$ can be bounded by,

$$S(\Lambda) \leq \frac{1}{T_N^{(M)}(\mathcal{X})} \tilde{R}_N \lesssim \frac{1}{n_\Lambda} \tilde{R}_{n_\Lambda}. \quad (9)$$

These intuitions will be more lucid in the discrete proofs than in the continuous case. In the latter, the set \mathcal{Z} will be dilated slightly to \mathcal{Z}_Λ where the dilation shrinks with Λ ; i.e. $\mathcal{Z}_\Lambda \rightarrow \mathcal{Z}$ as $\Lambda \rightarrow \infty$. This dilation appears due to a covering argument when extending some discrete proofs to continuous \mathcal{X} .

For our analysis, we will need to control the sum of conditional standard deviations for queries in a subset $A \subset \mathcal{X}$. We provide the lemma below, whose gist is borrowed from Srinivas et al. (2010).

Lemma 8 *Let $f \sim \mathcal{GP}(0, \kappa)$, $f : \mathcal{X} \rightarrow \mathbb{R}$ and each time we query at any $x \in \mathcal{X}$ we observe $y = f(x) + \epsilon$, where $\epsilon \sim \mathcal{N}(0, \eta^2)$. Let $A \subset \mathcal{X}$. Assume that we have queried f at n points, $(x_t)_{t=1}^n$ of which s points are in A . Let σ_{t-1} denote the posterior variance at time t , i.e. after $t - 1$ queries. Then, $\sum_{x_t \in A} \sigma_{t-1}^2(x_t) \leq \frac{2}{\log(1+\eta^{-2})} \Psi_s(A)$.*

Proof Let $A_s = \{z_1, z_2, \dots, z_s\}$ be the queries inside A in the order they were queried. Now, assuming that we have only queried inside A at A_s , denote by $\tilde{\sigma}_{t-1}(\cdot)$, the posterior standard deviation after $t - 1$ such queries. Then,

$$\begin{aligned} \sum_{t: x_t \in A} \sigma_{t-1}^2(x_t) &\leq \sum_{t=1}^s \tilde{\sigma}_{t-1}^2(z_t) \leq \sum_{t=1}^s \eta^2 \frac{\tilde{\sigma}_{t-1}^2(z_t)}{\eta^2} \leq \sum_{t=1}^s \frac{\log(1 + \eta^{-2} \tilde{\sigma}_{t-1}^2(z_t))}{\log(1 + \eta^{-2})} \\ &\leq \frac{2}{\log(1 + \eta^{-2})} I(y_{A_s}; f_{A_s}) \end{aligned}$$

Queries outside A will only decrease the variance of the GP so we can upper bound the first sum by the posterior variances of the GP with only the queries in A . The third step uses the inequality $u^2/v^2 \leq \log(1 + u^2)/\log(1 + v^2)$ with $u = \tilde{\sigma}_{t-1}(z_t)/\eta$ and $v = 1/\eta$ and the last step uses Lemma 15 in Appendix B.1. The result follows from the fact that $\Psi_s(A)$ maximises the mutual information among all subsets of size s . \blacksquare

8.1 Discrete \mathcal{X} :

Proof of Theorem 6. We will consider MF-GP-UCB after n steps and control the number of evaluations at different fidelities in different regions of the place. This will allow us to bound, among other things, the total number of plays N within capital Λ and the number of M^{th} fidelity evaluations outside $\bar{\mathcal{Z}}$. We will need the following two lemmas for our analysis. Lemma 9 is used to establish that $\varphi_t(x)$ upper bounds $f^{(M)}(x)$. Lemma 10 bounds $T_n^{(m)}(x)$ for different x, m . The proofs are given in Sections 8.1.1 and 8.1.2 respectively.

Lemma 9 *Pick $\delta \in (0, 1)$ and choose $\beta_t = 2 \log \left(\frac{M|\mathcal{X}|\pi^2 t^2}{3\delta} \right)$. Then, with probability at least $1 - \delta/2$, for all $t \geq 1$, for all $x \in \mathcal{X}$ and for all $m \in \{1, \dots, M\}$, we have*

$$|f^{(m)}(x) - \mu_{t-1}^{(m)}(x)| \leq \beta_t^{1/2} \sigma_{t-1}^{(m)}(x).$$

	$\mathcal{H}^{(1)}$	$\mathcal{H}^{(2)}$	$\mathcal{H}^{(m)}$	$\mathcal{H}^{(M)} \setminus \{x_\star\}$
$T_n^{(1)}(x)$	$\frac{5\eta^2}{\Delta^{(m)}(x)^2}\beta_n + 1$	$\frac{\eta^2}{\gamma^{(1)^2}\beta_n + 1}$	$\dots \frac{\eta^2}{\gamma^{(1)^2}\beta_n + 1} \dots$	$\frac{\eta^2}{\gamma^{(1)^2}\beta_n + 1}$
$T_n^{(2)}(x)$	n^α	$\frac{5\eta^2}{\Delta^{(m)}(x)^2}\beta_n + 1$	$\dots \frac{\eta^2}{\gamma^{(2)^2}\beta_n + 1} \dots$	$\frac{\eta^2}{\gamma^{(2)^2}\beta_n + 1}$
\vdots $T_n^{(m)}(x)$ \vdots		n^α	$\dots \frac{5\eta^2}{\Delta^{(m)}(x)^2}\beta_n + 1 \dots$	$\frac{\eta^2}{\gamma^{(m)^2}\beta_n + 1}$
$T_n^{(M)}(x)$			n^α	$\frac{5\eta^2}{\Delta^{(m)}(x)^2}\beta_n + 1$

Table 1: Bounds on the number of queries for each $x \in \mathcal{H}^{(m)}$ (columns) at each fidelity (rows). The bound for $T_n^{(M)}(x)$ in $\mathcal{H}^{(M)}$ holds for all arms except the optimal arm x_\star (note $\Delta^{(M)}(x_\star) = 0$).

Lemma 10 Pick $\delta \in (0, 1)$ and set $\beta_t = 2 \log \left(\frac{M|\mathcal{X}|\pi^2 t^2}{3\delta} \right)$. Let $\rho \geq 2$. Further assume $\varphi_t(x_\star) \geq f_\star$. Consider any $x \in \mathcal{H}^{(m)} \setminus \{x_\star\}$ for $m < M$. We then have the following bounds on the number of queries at any given time step n ,

$$T_n^{(\ell)}(x) \leq \frac{\eta^2}{\gamma^{(m)^2}\beta_n + 1}, \quad \text{for } \ell < m,$$

$$\mathbb{P} \left(T_n^{(m)}(x) > \left\lceil 5 \left(\frac{\eta}{\Delta^{(m)}(x)} \right)^2 \beta_n \right\rceil \right) \leq \frac{3\delta}{2\pi^2} \frac{1}{|\mathcal{X}|n^2},$$

$$\mathbb{P} \left(T_n^{(>m)}(x) > u \right) \leq \frac{3\delta}{2\pi^2} \frac{1}{|\mathcal{X}|u^{2(\rho-1)^2-1}}.$$

First whenever $\varphi_t(x_\star) \geq f_\star$, by using the union bound on the second result of Lemma 10,

$$\mathbb{P} \left(\forall n \geq 1, \forall m \in \{1, \dots, M\}, \forall x \in \mathcal{H}^{(m)} \setminus \{x_\star\}, T_n^{(m)}(x) > \left\lceil 5 \left(\frac{\eta}{\Delta^{(m)}(x)} \right)^2 \beta_n \right\rceil \right) \leq \frac{\delta}{4}.$$

Here we have used $\sum n^{-2} = \pi^2/6$. The last two quantifiers just enumerates over all $x \in \mathcal{X} \setminus \{x_\star\}$. Next, in the third result of Lemma 10 we use $u = n^\alpha$ and $\rho = 1 + \sqrt{1/2 + 1/\alpha}$ as given in the theorem. Then, $u^{2(\rho-1)^2-1} = n^2$. Applying the union bound over $n \geq 1$ we have,

$$\mathbb{P} \left(\forall n \geq 1, \forall m \in \{1, \dots, M\}, \forall x \in \mathcal{H}^{(m)}, T_n^{(>m)}(x) > n^\alpha \right) \leq \frac{\delta}{4}$$

The condition for Lemma 10 holds with probability $> 1 - \delta/2$ (by Lemma 9), and the above bounds hold together with probability $> 1 - \delta$. We have tabulated these bounds in Table 1. We can read off the following bound for the number of fidelity m ($< M$) plays $T_n^{(m)}(\mathcal{X})$ from the table,

$$T_n^{(m)}(\mathcal{X}) \leq |\tilde{\mathcal{H}}^{(m)}|n^\alpha + \sum_{x \in \mathcal{H}^{(m)}} \frac{5\eta^2}{\Delta^{(m)}(x)^2}\beta_n + 1 + |\hat{\mathcal{H}}^{(m)}| \left(\frac{\eta^2}{\gamma^{(m)^2} \log(n) + 1} \right).$$

Now we can control the number of evaluations at the approximations. Precisely, we will prove the following bound on the number of plays at fidelities less than M .

$$\sum_{m=1}^{M-1} \sum_{x \in \mathcal{X}} T_n^{(m)}(x) \leq |\mathcal{X}|n^\alpha + \sum_{m=1}^{M-1} \sum_{x \in \mathcal{H}^{(m)}} \left(\frac{5\eta^2}{\Delta^{(m)}(x)^2} \beta_n + 1 \right) + \sum_{m=1}^{M-1} |\widehat{\mathcal{H}}^{(m)}| \left(\frac{\eta^2}{\gamma^{(m)2}} \beta_n + 1 \right). \quad (10)$$

For this we first note that the LHS of (10) is reducible to the following for all $m \leq M - 1$,

$$\sum_{x \in \mathcal{X}} T_n^{(m)}(x) \leq \sum_{x \in \check{\mathcal{H}}^{(m)}} T_n^{(m)}(x) + \sum_{x \in \mathcal{H}^{(m)}} \left(\frac{5\eta^2}{\Delta^{(m)}(x)^2} \beta_n + 1 \right) + \sum_{x \in \check{\mathcal{H}}^{(m)}} \left(\frac{\eta^2}{\gamma^{(m)2}} \beta_n + 1 \right).$$

Now summing the above from $m = 1$ to $M - 1$ and rearranging the $T_n^{(>m)}(x)$ terms as follows gives us the bound (10).

$$\sum_{m=1}^{M-1} \sum_{x \in \check{\mathcal{H}}^{(m)}} T_n^{(m)}(x) = \sum_{m=1}^{M-1} \sum_{\ell=1}^{m-1} \sum_{x \in \mathcal{H}^{(\ell)}} T_n^{(m)}(x) \leq \sum_{m=1}^{M-2} \sum_{x \in \mathcal{H}^{(m)}} T_n^{(>m)}(x) \leq |\mathcal{X}|n^\alpha. \quad (11)$$

Since $\beta_n \in \mathcal{O}(\log(n))$ the RHS of (10) is sublinear in n . Say we have queried an n_0 number of times such that for all $n \geq n_0$, this bound is less than $n/2$. For all such n , $T_n^{(M)}(\mathcal{X}) > n/2$ and therefore the expended budget after n rounds $\Lambda(n)$ satisfies $\Lambda(n) \geq \lambda^{(M)}n/2$. Since our bounds hold with probability $> 1 - \delta$ for all n we can invert the above inequality to bound the number of random plays N after some capital Λ ; i.e. $N \leq 2\Lambda/\lambda^{(M)} \leq 2n_\Lambda$. We only need to make sure that $N \geq n_0$ which can be guaranteed if $\Lambda \geq \Lambda_0 := \lambda^{(M)}(n_0 + 1)$ since $N \geq \lfloor \Lambda/\lambda^{(M)} \rfloor$.

We now proceed to bound the terms $\tilde{R}_{n,1}, \tilde{R}_{n,2}$. First note the following bound on the instantaneous regret.

$$\begin{aligned} f_\star - f^{(M)}(x_t) &\leq \varphi_t(x_\star) - (\mu_{t-1}^{(M)}(x_t) - \beta_t^{1/2} \sigma_{t-1}^{(M)}(x_t)) \\ &\leq \varphi_t(x_t) - (\mu_{t-1}^{(M)}(x_t) - \beta_t^{1/2} \sigma_{t-1}^{(M)}(x_t)) \leq 2\beta_t^{1/2} \sigma_{t-1}^{(M)}(x_t) \end{aligned} \quad (12)$$

The first step uses that $\varphi_t^{(m)}(x)$ is an upper bound for $f^{(M)}(x)$ by Lemma 9 and the assumption **A2**, and hence so is the minimum $\varphi_t(x)$. The second step uses that x_t was the maximiser of $\varphi_t(x)$ and the third step that $\varphi_t^{(M)}(x) \geq \varphi_t(x)$.

To control $\tilde{R}_{n,1}, \tilde{R}_{n,2}$ we will use $\mathcal{Z} = \mathcal{H}^{(M)}$ and $\bar{\mathcal{Z}} = \bar{\mathcal{H}}^{(M)} = \check{\mathcal{H}}^{(M)}$ in (8) and invoke Lemma 8. Applying Jensen's inequality in the form $(\sum_{i=1}^s a_i)^2 \leq s \sum_{i=1}^s a_i^2$ yields,

$$\begin{aligned} \tilde{R}_{n,2}^2 &\leq T_n^{(m)}(\bar{\mathcal{Z}}) \sum_{\substack{t:m_t=M \\ x_t \in \bar{\mathcal{Z}}}} \left(f_\star - f^{(M)}(x_t) \right)^2 \leq T_n^{(m)}(\bar{\mathcal{Z}}) \sum_{\substack{t:m_t=M \\ x_t \in \bar{\mathcal{Z}}}} 4\beta_t (\sigma_{t-1}^{(m)}(x_t))^2 \\ &\leq C_1 T_n^{(m)}(\bar{\mathcal{Z}}) \beta_n \Psi_{T_n^{(m)}(\bar{\mathcal{Z}})}(\bar{\mathcal{Z}}) \end{aligned} \quad (13)$$

where $C_1 = 8/\log(1 + \eta^{-2})$. Once again, using Table 1 we can bound $T_n^{(M)}(\check{\mathcal{H}}^{(M)}) \leq |\check{\mathcal{H}}^{(M)}|n^\alpha \leq |\mathcal{X}|n^\alpha$. Therefore we have $\tilde{R}_{n,3} \leq \sqrt{|\mathcal{X}|^\alpha C_1 n^\alpha \beta_n \Psi_{(|\mathcal{X}|n^\alpha)}(\mathcal{X})}$. Bounding $\tilde{R}_{n,2}$ follows essentially a similar procedure. Since $T_n^{(m)}(\mathcal{H}^{(m)}) \leq n$ trivially, we have $\tilde{R}_{n,2} \leq \sqrt{C_1 n \beta_n \Psi_n(\mathcal{X})}$.

Recall that $N \leq 2n_\Lambda$ when $\Lambda \geq \Lambda_0$. Using this result along with (8) bounds \tilde{R}_N . The theorem follows by noting that $N \geq n_\Lambda$ trivially, and using it in (9) to bound the simple regret $S(\Lambda)$. \blacksquare

Some Remarks

1. Since the switching criterion of MF-GP-UCB (step 2 in Algorithm 2) makes sure that we do not query often at a lower fidelity, an easy upper bound for $T_n^{(m)}(x)$ is $\frac{\eta^2}{\gamma^{(m)^2}}\beta_n + 1$. While we have used this to bound the number of plays in $\hat{\mathcal{H}}^{(m)}$ we have used different techniques for the points in $\mathcal{H}^{(m)}, \check{\mathcal{H}}^{(m)}$. The main reason is to avoid the $1/\gamma^{(m)^2}$ dependence on these arms. In particular, we can control the number of plays at the m^{th} fidelity for any $x \in \mathcal{H}^{(m)}$ using the difference $\Delta^{(m)}(x)$. For x far away from the optimum this provides a tighter bound.
2. A polylog(n_Λ) rate can also be shown for the discrete case, similar to Theorem 1 in Dani et al. (2008), but it will have worse dependence on Ψ . We stick to the above form which is comparable to the results of Srinivas et al. (2010).

8.1.1 PROOF OF LEMMA 9

This is a straightforward argument using Gaussian concentration and the union bound. But we would like to emphasise a subtle conditioning argument with multiple fidelities. Consider any given m, t, x .

$$\begin{aligned} \mathbb{P}\left(|f^{(m)}(x) - \mu_{t-1}^{(m)}(x)| > \beta_t^{1/2} \sigma_{t-1}^{(m)}(x)\right) &= \mathbb{E}\left[\mathbb{E}\left[|f^{(m)}(x) - \mu_{t-1}^{(m)}(x)| > \beta_t^{1/2} \sigma_{t-1}^{(m)}(x) \mid \mathcal{D}_{t-1}^{(m)}\right]\right] \\ &= \mathbb{E}\left[\mathbb{P}_{Z \sim \mathcal{N}(0,1)}\left(|Z| > \beta_t^{1/2}\right)\right] \\ &\leq \exp\left(\frac{\beta_t}{2}\right) = \frac{3\delta}{M|\mathcal{X}|\pi^2 t^2}. \end{aligned}$$

In the first step we have conditioned w.r.t $\mathcal{D}_{t-1}^{(m)}$ which allows us to use Lemma 14. The posterior conditioned on all queries will not be a Gaussian due to the $\zeta^{(m)}$ constraints. We will be using this conditioning argument repeatedly in our analysis. The statement follows via a union bound over all $m \in \{1, \dots, M\}, x \in \mathcal{X}$ and all t and noting that $\sum_t t^{-2} = \pi^2/6$. \blacksquare

8.1.2 PROOF OF LEMMA 10

First consider any $\ell < m$. Assume that we have already queried $\eta^2 \beta_n / \gamma^{(m)^2} + 1$ times at any $t \leq n$. Since the Gaussian variance after s observations is η^2/s and that queries elsewhere will only decrease the conditional variance we have, $\kappa_{t-1}^{(\ell)}(x, x) \leq \eta^2/T_{t-1}^{(\ell)}(x) < \gamma^{(m)^2}/\beta_n$. Therefore, $\beta_t^{1/2} \sigma_{t-1}^{(\ell)}(x) < \beta_n^{1/2} \sigma_{t-1}^{(\ell)}(x) < \gamma^{(m)}$ and by the design of our algorithm we will not play at the ℓ^{th} fidelity at time t for all t until n . This establishes the first result.

To bound $T_n^{(m)}(x)$ we first observe,

$$\begin{aligned} \mathbb{1}\{T_n^{(m)}(x) > u\} &\leq \mathbb{1}\{\exists t : u + 1 \leq t \leq n : \varphi_t(x) \text{ was maximum} \wedge \\ &\quad \beta_t^{1/2} \sigma_{t-1}^{(\ell)}(x) < \gamma^{(m)}, \forall \ell < m \wedge \beta_t^{1/2} \sigma_{t-1}^{(m)}(x) \geq \gamma^{(m)} \wedge T_{t-1}^{(m)}(x) \geq u\} \\ &\leq \mathbb{1}\{\exists t : u + 1 \leq t \leq n : \varphi_t(x) > \varphi_t(x_\star) \wedge T_{t-1}^{(m)}(x) \geq u\} \\ &\leq \mathbb{1}\{\exists t : u + 1 \leq t \leq n : \varphi_t^{(m)}(x) > f_\star \wedge T_{t-1}^{(m)}(x) \geq u\}. \end{aligned} \quad (14)$$

The first line just enumerates the conditions in our algorithm for it to have played x at time t at fidelity m . In the second step we have relaxed some of those conditions, noting in particular that if $\varphi_t(\cdot)$ was maximised at x then it must be larger than $\varphi_t(x_*)$. The last step uses the fact that $\varphi_t^{(m)}(x) \geq \varphi_t(x)$ and the assumption on $\varphi_t(x_*)$. Consider the event $\{\varphi_t^{(m)}(x) > f_* \wedge T_{t-1}^{(m)}(x) \geq u\}$. We will choose $u = \lceil 5\eta^2\beta_n/\Delta^{(m)}(x)^2 \rceil$ and bound its probability via,

$$\begin{aligned}
 & \mathbb{P}\left(\varphi_t^{(m)}(x) > f_* \wedge T_{t-1}^{(m)}(x) \geq u\right) \\
 &= \mathbb{P}\left(\mu_{t-1}^{(m)}(x) + \beta_t^{1/2}\sigma_{t-1}^{(m)}(x) + \zeta^{(m)} > f_* \quad \wedge \quad T_{t-1}^{(m)}(x) \geq u\right) \\
 &= \mathbb{P}\left(\mu_{t-1}^{(m)}(x) - f^{(m)}(x) > \underbrace{f_* - f^{(m)}(x) - \zeta^{(m)}}_{\Delta^{(m)}(x)} - \beta_t^{1/2}\sigma_{t-1}^{(m)}(x) \quad \wedge \quad T_{t-1}^{(m)}(x) > u\right) \\
 &\leq \mathbb{P}\left(\mu_{t-1}^{(m)}(x) - f^{(m)}(x) > (\sqrt{5} - 1)\beta_n^{1/2}\sigma_{t-1}^{(m)}(x)\right) \\
 &\leq \mathbb{P}_{Z \sim \mathcal{N}(0,1)}\left(Z > \frac{(\sqrt{5} - 1)^2}{2}\beta_n^{1/2}\right) \leq \frac{1}{2} \exp\left(-\frac{3}{4}\beta_n\right) \\
 &= \frac{1}{2} \left(\frac{3\delta}{M|\mathcal{X}|\pi^2}\right)^{\frac{3}{2}} n^{-3} \leq \frac{1}{2} \frac{3\delta}{|\mathcal{X}|\pi^2} n^{-3}
 \end{aligned}$$

Above in the third step we have used, if $u \geq 5\eta^2\beta_n/\Delta^{(m)}(x)^2$, then $\Delta^{(m)}(x) \geq \sqrt{5}\beta_n^{1/2}\sigma_{t-1}^{(m)}(x)$ and that $\beta_n \geq \beta_t$. The fourth step uses Lemma 14 after conditioning on $\mathcal{D}_{t-1}^{(m)}$, the fifth step uses $(\sqrt{5} - 1)^2 > 3/2$ and the last step uses $3\delta/|\mathcal{X}|\pi^2 < 1$. Now use the union bound on (14), $\mathbb{P}(T_n^{(m)}(x) > u) \leq \sum_{t=u+1}^n \mathbb{P}(\varphi_t^{(m)}(x) > f_* \wedge T_{t-1}^{(m)}(x) \geq u)$. The second inequality of the theorem follows by noting that there are at most n terms in the summation.

Finally, for the third inequality we observe

$$\mathbb{P}(T_n^{(>m)}(x) > u) \leq \mathbb{P}(\exists t : u + 1 \leq t \leq n; \varphi_t^{(m)}(x) > f_* \quad \wedge \quad \beta_t^{1/2}\sigma_{t-1}^{(m)}(x) < \gamma^{(m)}). \quad (15)$$

As before, we have used that if x is to be queried at time t , then $\varphi_t(x)$ should be at least larger than $\varphi_t(x_*)$ which is larger than f_* due to the assumption in the theorem. The second condition is necessary to ensure that the switching procedure proceeds beyond the m^{th} fidelity. It is also necessary to have $\beta_t^{1/2}\sigma_{t-1}^{(\ell)}(x) < \gamma^{(\ell)}$ for $\ell < m$, but we have relaxed them. We first bound the probability of the event $\{\varphi_t^{(m)}(x) > f_* \quad \wedge \quad \beta_t^{1/2}\sigma_{t-1}^{(m)}(x) < \gamma^{(m)}\}$.

$$\begin{aligned}
 & \mathbb{P}(\varphi_t^{(m)}(x) > f_* \wedge \beta_t^{1/2}\sigma_{t-1}^{(m)}(x) < \gamma^{(m)}) \\
 &= \mathbb{P}(\mu_{t-1}^{(m)}(x) - f^{(m)}(x) > \Delta^{(m)}(x) - \beta_t^{1/2}\sigma_{t-1}^{(m)}(x) \quad \wedge \quad \beta_t^{1/2}\sigma_{t-1}^{(m)}(x) < \gamma^{(m)}) \\
 &\leq \mathbb{P}(\mu_{t-1}^{(m)}(x) - f^{(m)}(x) > \rho\gamma^{(m)} - \beta_t^{1/2}\sigma_{t-1}^{(m)}(x) \quad \wedge \quad \beta_t^{1/2}\sigma_{t-1}^{(m)}(x) < \gamma^{(m)}) \\
 &\leq \mathbb{P}(\mu_{t-1}^{(m)}(x) - f^{(m)}(x) > (\rho - 1)\beta_t^{1/2}\sigma_{t-1}^{(m)}(x)) \leq \mathbb{P}_{Z \sim \mathcal{N}(0,1)}\left(Z > (\rho - 1)\beta_t^{1/2}\right) \\
 &\leq \frac{1}{2} \exp\left(-\frac{(\rho - 1)^2}{2}\beta_t\right) = \frac{1}{2} \left(\frac{3\delta}{M|\mathcal{X}|\pi^2}\right)^{(\rho-1)^2} t^{-2(\rho-1)^2} \leq \frac{1}{2} \frac{3\delta}{|\mathcal{X}|\pi^2} t^{-2(\rho-1)^2}
 \end{aligned}$$

Here, the second step uses that for all $x \in \mathcal{H}^{(m)}$, $\Delta^{(m)}(x) > \rho\gamma^{(m)}$. The third step uses the second condition and the last step uses that $\rho \geq 2$. Using the union bound on (15) and bounding the sum by

an integral gives us,

$$\begin{aligned} \mathbb{P}(T_n^{(>m)}(x) > u) &\leq \sum_{t=u+1}^n \frac{1}{2} \frac{3\delta}{|\mathcal{X}| \pi^2} t^{-2(\rho-1)^2} \leq \frac{1}{2} \frac{3\delta}{|\mathcal{X}| \pi^2} \int_u^\infty t^{-2(\rho-1)^2} dt \\ &\leq \frac{1}{2} \frac{3\delta}{|\mathcal{X}| \pi^2} \frac{1}{u^{2(\rho-1)^2-1}}. \end{aligned}$$

■

8.2 Compact and Convex \mathcal{X}

To prove theorem 7 we will require a fairly delicate set up for the continuous setting. We will denote the ε covering number of a set $A \subset \mathcal{X}$ in the $\|\cdot\|_2$ metric by $\Omega_\varepsilon(A)$. For the analysis, at time n we will consider a $\frac{r\sqrt{d}}{2n^{\frac{\alpha}{2d}}}$ -covering of the space \mathcal{X} of size $n^{\frac{\alpha}{2}}$. For instance, if $\mathcal{X} = [0, r]^d$ a sufficient discretisation would be an equally spaced grid having $n^{\alpha/2d}$ points per side. Let $\{a_{i,n}\}_{i=1}^{n^{\frac{\alpha}{2}}}$ be the points in the covering, $F_n = \{A_{i,n}\}_{i=1}^{n^{\frac{\alpha}{2}}}$ be the ‘‘cells’’ in the covering, i.e. $A_{i,n}$ is the set of points which are closest to $a_{i,n}$ in \mathcal{X} and the union of all sets $A_{i,n}$ in F_n is \mathcal{X} . Next we will define another partitioning of the space similar in spirit to (6) using this covering. First let $F_n^{(1)} = \{A_{i,n} \in F_n : A_{i,n} \subset \mathcal{J}_{\max(\tau, \rho\gamma)}^{(1)}\}$. Next,

$$F_n^{(m)} = \left\{ A_{i,n} \in F_n : A_{i,n} \subset \overline{\mathcal{J}}_{\max(\tau, \rho\gamma)}^{(m)} \wedge A_{i,n} \notin \bigcup_{\ell=1}^{m-1} F_n^{(\ell)} \right\} \text{ for } 2 \leq m \leq M-1. \quad (16)$$

We define the following *disjoint* subsets $\{\mathcal{F}_n^{(m)}\}_{m=1}^{M-1}$ of \mathcal{X} via $\mathcal{F}_n^{(m)} = \bigcup_{A_{i,n} \in F_n^{(m)}} A_{i,n}$. We have illustrated $\bigcup_{\ell=1}^{m-1} \mathcal{F}_n^{(\ell)}$ with respect to $\mathcal{H}_\tau^{(m)}$ and $\widehat{\mathcal{H}}_\tau^{(m)}$ in Figure 8. By observing that $\mathcal{H}_{\tau,n}^{(1)} = \mathcal{H}^{(1)}$ and that $\mathcal{H}_{\tau,n}^{(m)} \cup \widehat{\mathcal{H}}^{(m)} \subset \bigcup_{\ell=1}^{m-1} \mathcal{F}_n^{(\ell)}$ (see Figure 8) we have the following,

$$\forall m \in \{1, \dots, M\}, \quad T_n^{(m)}(\mathcal{X}) \leq \left(\sum_{\ell=1}^{m-1} T_n^{(m)}(\mathcal{F}_n^{(\ell)}) \right) + T_n^{(m)}(\mathcal{H}_{\tau,n}^{(m)}) + T_n^{(m)}(\widehat{\mathcal{H}}^{(m)}). \quad (17)$$

We are now ready to prove Theorem 7.

Proof of Theorem 7. As in the discrete case, we will proceed to control the number of lower fidelity evaluations by controlling each term in (17). First we focus on $\widehat{\mathcal{H}}^{(m)}$ for which we use the following lemma. The proof is given in Section 8.2.1.

Lemma 11 *Let $f \sim \mathcal{GP}(\mathbf{0}, \kappa)$, $f : \mathcal{X} \rightarrow \mathbb{R}$ and we observe $y = f(x) + \epsilon$ where $\epsilon \sim \mathcal{N}(0, \eta^2)$. Let $A \subset \mathcal{X}$ such that its L_2 diameter $\text{diam}(A) \leq D$. Say we have n queries $(x_t)_{t=1}^n$ of which s points are in A . Then the posterior variance of the GP, $\kappa'(x, x)$ at any $x \in A$ satisfies*

$$\kappa'(x, x) \leq \begin{cases} C_{SE} D^2 + \frac{\eta^2}{s} & \text{if } \kappa \text{ is the SE kernel,} \\ C_{Mat} D + \frac{\eta^2}{s} & \text{if } \kappa \text{ is the Matérn kernel,} \end{cases}$$

for appropriate constants C_{SE}, C_{Mat} .

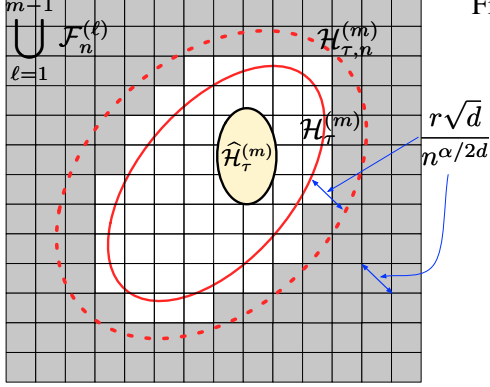


Figure 8: Illustration of the sets $\{\mathcal{F}_n^{(\ell)}\}_{\ell=1}^{m-1}$ with respect to $\mathcal{H}_\tau^{(m)}$. The grid represents a $r\sqrt{d}/n^{\alpha/2d}$ covering of \mathcal{X} . The yellow region is $\widehat{\mathcal{H}}_\tau^{(m)}$. The area enclosed by the solid red line (excluding $\widehat{\mathcal{H}}_\tau^{(m)}$) is $\mathcal{H}_\tau^{(m)}$. $\mathcal{H}_{\tau,n}^{(m)}$, shown by a dashed red line, is obtained by dilating $\mathcal{H}_\tau^{(m)}$ by $r\sqrt{d}/n^{\alpha/2d}$. The grey shaded region represents $\bigcup_{\ell=1}^{m-1} \mathcal{F}_n^{(\ell)}$. By our definition, $\bigcup_{\ell=1}^{m-1} \mathcal{F}_n^{(\ell)}$ contains the cells which are entirely outside $\mathcal{H}_\tau^{(m)}$. However, the inflation $\mathcal{H}_{\tau,n}^{(m)}$ is such that $\widehat{\mathcal{H}}_\tau^{(m)} \cup \mathcal{H}_{\tau,n}^{(m)} \cup \bigcup_{\ell=1}^{m-1} \mathcal{F}_n^{(\ell)} = \mathcal{X}$. We further note that as $n \rightarrow \infty$, $\mathcal{H}_{\tau,n}^{(m)} \rightarrow \mathcal{H}_\tau^{(m)}$.

First consider the SE kernel. At time t consider any $\varepsilon_n = \frac{\gamma^{(m)}}{\sqrt{8C_{SE}\beta_n}}$ covering $(B_i)_{i=1}^{\varepsilon_n}$ of $\widehat{\mathcal{H}}_\tau^{(m)}$. The number of queries inside any B_i of this covering at time n will be at most $\frac{2\eta^2}{\gamma^{(m)^2}\beta_n} + 1$. To see this, assume we have already queried $2\eta^2/\gamma^{(m)^2} + 1$ times inside B_i at time $t \leq n$. By Lemma 11 the maximum variance in A_i can be bounded by

$$\max_{x \in A_i} \kappa_{t-1}^{(m)}(x, x) \leq C_{SE}(2\varepsilon_n)^2 + \frac{\eta^2}{T_t^{(m)}(A_i)} < \frac{\gamma^{(m)^2}}{\beta_n}.$$

Therefore, $\beta_t^{1/2}\sigma_{t-1}^{(m)}(x) \leq \beta_n^{1/2}\sigma_{t-1}^{(m)}(x) < \gamma^{(m)}$ and we will not query inside A_i until time n . Therefore, the number of m^{th} fidelity queries is bounded by $\Omega_{\varepsilon_n}(\widehat{\mathcal{H}}_\tau^{(m)}) \left(\frac{2\eta^2}{\gamma^{(m)^2}\beta_n} + 1 \right)$. The proof for the Matérn kernel follows similarly using $\varepsilon_n = \frac{\gamma^{(m)^2}}{8C_{Mat}\beta_n}$. Next, we bound $T_n^{(m)}(\mathcal{H}_{\tau,n}^{(m)})$ for which we will use the following Lemma. The proof is given in Section 8.2.2.

Lemma 12 For β_t as given in Theorem 7, we have the following with probability $> 1 - 5\delta/6$.

$$\forall m \in \{1, \dots, M\}, \quad \forall t \geq 1, \quad \Delta^{(m)}(x_t) = f_\star - f^{(m)}(x_t) \leq 2\beta_t\sigma_{t-1}^{(m)}(x_t) + 1/t^2.$$

We will analyse the quantity $\tilde{R}_n^{(m)}$ for $m < M$ defined and bounded below using Lemma 12.

$$\tilde{R}_n^{(m)} \triangleq \sum_{\substack{t:m_t=m \\ x_t \in \mathcal{H}_{\tau,n}^{(m)}}} \Delta^{(m)}(x_t) \leq 2\beta_n^{1/2} \cdot \sum_{\substack{t:m_t=m \\ x_t \in \mathcal{H}_{\tau,n}^{(m)}}} \sigma_{t-1}^{(m)}(x_t) + \frac{\pi^2}{6}$$

Then, using Lemma 8 and Jensen's inequality we have,

$$\begin{aligned} \left(\tilde{R}_n^{(m)} - \frac{\pi^2}{6} \right)^2 &\leq 4\beta_t T_n^{(m)}(\mathcal{H}_{\tau,n}^{(m)}) \sum_{\substack{t:m_t=m \\ x_t \in \mathcal{H}_{\tau,n}^{(m)}}} (\sigma_{t-1}^{(m)})^2(x_t) \\ &\leq C_1\beta_t T_n^{(m)}(\mathcal{H}_{\tau,n}^{(m)}) \Psi_{T_n^{(m)}(\mathcal{H}_{\tau,n}^{(m)})}(\mathcal{H}_{\tau,n}^{(m)}). \end{aligned} \quad (18)$$

We therefore have, $\tilde{R}_n^{(m)} \leq \sqrt{C_1 n \beta_n \Psi_n(\mathcal{H}_{\tau,n}^{(m)})} + \pi^2/6$ since trivially $T_n^{(m)}(\mathcal{H}_{\tau,n}^{(m)}) < n$. However, since $\Delta^{(m)}(x) > \tau$ for $x \in \mathcal{H}_{\tau,n}^{(m)}$ we have $T_n^{(m)}(\mathcal{H}_{\tau,n}^{(m)}) < \frac{1}{\tau} \left(\sqrt{C_1 n \beta_n \Psi_n(\mathcal{H}_{\tau,n}^{(m)})} + \pi^2/6 \right)$.

Finally, to control the first term in (17), we will bound $T_n^{(>m)}(\mathcal{F}_n^{(m)})$. To that end we provide the following Lemma. The proof is given in Section 8.2.3.

Lemma 13 Consider any $A_{i,n} \in F_n^{(m)}$ where $F_n^{(m)}$ is as defined in (16) for any $\alpha \in (0, 1)$. Let ρ, β_t be as given in Theorem 7, Then for all $u \geq \max\{3, (2(\rho - \rho_0)\eta)^{-2/3}\}$ we have,

$$\mathbb{P}(T_n^{(>m)}(A_{i,n}) > u) \leq \frac{\delta}{\pi^2} \cdot \frac{1}{u^{1+4/\alpha}}$$

We will use the above result with $u = n^{\alpha/2}$. Applying the union bound over all $m \in \{1, \dots, M\}$ and $A_{i,n} \in F_n^{(m)}$ we have,

$$\begin{aligned} \mathbb{P}\left(\forall m \in \{1, \dots, M\}, T_n^{(>m)}(\mathcal{F}_n^{(m)}) > |F_n^{(m)}| n^{\alpha/2}\right) &\leq \sum_{m=1}^M \mathbb{P}\left(T_n^{(>m)}(\mathcal{F}_n^{(m)}) > |F_n^{(m)}| n^{\alpha/2}\right) \\ &\leq \sum_{m=1}^M \sum_{A_{i,n} \in F_n^{(m)}} \mathbb{P}\left(T_n^{(>m)}(A_{i,n}) > n^{\alpha/2}\right) \leq \sum_{m=1}^M |F_n^{(m)}| \frac{\delta}{\pi^2} \frac{1}{n^{2+\alpha/2}} \\ &\leq |F_n| \frac{\delta}{\pi^2} \frac{1}{n^{2+\alpha/2}} = \frac{\delta}{\pi^2} \frac{1}{n^2}. \end{aligned}$$

Applying the union bound over n , we have $T_n^{(>m)}(\mathcal{F}_n^{(m)}) \leq n^\alpha$ for all m and all $n \geq \max\{3, (2(\rho - \rho_0)\eta)^{2/3}\}^{2/\alpha}$ with probability $> 1 - \delta/6$.

Henceforth, all statements we make will make use of the results in Lemmas 11, 12 and 13 and will hold with probability $> 1 - \delta$. Using (17) and noting $T_n^{(m)}(\mathcal{F}_n^{(\ell)}) \leq T_n^{(>\ell)}(\mathcal{F}_n^{(\ell)})$ for $\ell < m$ we can bound the number of m^{th} fidelity evaluations $T_n^{(m)}(\mathcal{X})$ for $m < M$.

$$T_n^{(m)}(\mathcal{X}) \leq (m-1)n^\alpha + \frac{1}{\tau} \left(\sqrt{C_1 n \beta_n \Psi_n(\mathcal{H}_{\tau,n}^{(m)})} + \frac{\pi^2}{6} \right) + \Omega_{\varepsilon_n}(\hat{\mathcal{H}}^{(m)}) \left(\frac{2\eta^2}{\gamma^{(m)2} \beta_n} + 1 \right).$$

Using a similar reasoning to (10) and (11), we can show that the following term upper bounds the number of queries at fidelities less than M ,

$$\begin{aligned} \sum_{m=1}^{M-1} \sum_{x \in \mathcal{X}} T_n^{(m)}(x) &\leq (M-1)n^\alpha + \sum_{m=1}^{M-1} \frac{1}{\tau} \left(\sqrt{2C_1 n \beta_n \Psi_n(\mathcal{H}_{\tau,n}^{(m)})} + \frac{\pi^2}{6} \right) \\ &\quad + \sum_{m=1}^{M-1} \Omega_{\varepsilon_n}(\hat{\mathcal{H}}^{(m)}) \left(\frac{2\eta^2}{\gamma^{(m)2} \beta_n} + 1 \right). \end{aligned} \quad (19)$$

Assume n_0 is large enough so that $n_0 \geq \max\{3, (2(\rho - \rho_0)\eta)^{-2/3}\}^{2/\alpha}$ and for all $n \geq n_0$, $n/2$ is larger than the above upper bound. We can find such an n_0 since the RHS of (19) is sublinear in

n . Therefore, for all $n \geq n_0$, $T_n^{(M)}(\mathcal{X}) > n/2$. Following a similar argument to the discrete case, $N \leq 2\Lambda/\lambda^{(M)}$ with probability $> 1 - \delta$ if $\Lambda \geq \Lambda_0 = \lambda^{(M)}(n_0 + 1)$.

We now proceed to bound $\tilde{R}_{n,1}, \tilde{R}_{n,2}$ in (8) for which we set $\mathcal{Z} = \mathcal{H}_{\tau, n_\Lambda}^{(M)}$. Using Lemma 12 and similar calculations to (18) and as $T_n^{(M)}(\mathcal{H}_{\tau, n}^{(m)}) \leq n$, we have

$$\tilde{R}_{n,1} \leq \sqrt{C_1 n \beta_n \Psi_n(\mathcal{H}_{\tau, n}^{(m)})} + \sum_{\substack{m_t=M \\ x_t \in \mathcal{Z}}} \frac{1}{t^2}.$$

Next, using Lemma 13 and observing $\bar{\mathcal{Z}} = \overline{\mathcal{H}_{\tau, n}^{(M)}} \subset \bigcup_{\ell=1}^{M-1} \mathcal{F}_n^{(m)} \subset \check{\mathcal{H}}^{(M)}$, we have,

$$\begin{aligned} \tilde{R}_{n,2} &= \sum_{\substack{t:m_t=M \\ x_t \in \bar{\mathcal{Z}}}} (f_\star - f^{(M)}(x_t)) \leq \sum_{\substack{t:m_t=M \\ x_t \in \bigcup_{\ell=1}^{M-1} \mathcal{F}_n^{(m)}}} 2\beta_t^{1/2} \sigma_{t-1}^{(m)}(x_t) + \sum_{x_t \in \bar{\mathcal{Z}}} \frac{1}{t^2} \\ &\leq \sqrt{C_1 M n^\alpha \beta_n \Psi_{M n^\alpha}(\check{\mathcal{H}}^{(M)})} + \sum_{\substack{m_t=M \\ x_t \in \bar{\mathcal{Z}}}} \frac{1}{t^2}. \end{aligned}$$

We now observe $N \geq n_\Lambda \implies \mathcal{H}_{\tau, N}^{(m)} \subset \mathcal{H}_{\tau, n_\Lambda}^{(m)} \implies \Psi_N(\mathcal{H}_{\tau, N}^{(m)}) \leq \Psi_N(\mathcal{H}_{\tau, n_\Lambda}^{(m)}) \leq \Psi_{2n_\Lambda}(\mathcal{H}_{\tau, n_\Lambda}^{(m)})$. The theorem follows by noting $n_\Lambda \leq N \leq 2n_\Lambda$ and an application of (8) followed by (9). \blacksquare

Some Remarks

1. Since $\Psi_n(\cdot)$ is typically sublinear in n , it is natural to ask if we can recursively apply this to obtain a tighter bound on $T_n^{(m)}(\mathcal{H}_{\tau, n}^{(m)})$. For instance, since $\Psi_n(\cdot)$ is polylog(n) for the SE kernel (Srinivas et al. (2010), Theorem 5) by repeating the argument above once we get, $T_n^{(m)}(\mathcal{H}_{\tau, n}^{(m)}) \asymp \frac{1}{\tau^{3/2}} \sqrt{n^{1/2} \text{polylog}(n) \Psi_{n^{1/2}}(\mathcal{H}_{\tau, n}^{(m)})}$. However, while this improves the dependence on n it worsens the dependence on τ . In fact, using a discretisation argument similar to that in Lemma 13 and the variance bound in Lemma 11, a polylog(n)/poly(τ) bound can be shown, where poly(τ) is τ^{d+2} for the SE kernel and τ^{2d+2} for the Matérn kernel.
2. Λ_0 depends on n_0 and consequently on the RHS of (19) in which the covering number of $\hat{\mathcal{H}}^{(m)}$ appears. For the SE kernel, $\Omega_{\varepsilon_n}(\cdot) \asymp \text{vol}(\cdot) \log(n)^{1+d/2} / \gamma^{(m)d}$ and for the Matérn kernel, $\Omega_{\varepsilon_n}(\cdot) \asymp \text{vol}(\cdot) \log(n)^{1+d} / \gamma^{(m)2d}$. The first observation is that it scales with the volume of $\mathcal{H}^{(m)}$ which also grows at rate $\gamma^{(m)d}$. Therefore the dependence of the RHS of (19) on $\gamma^{(m)}$ is only $1/\gamma^{(m)2}$ as for the discrete case while for the Matérn kernel it has a worse $1/\gamma^{(m)d+2}$ dependence. Secondly, it also indicates that when the m^{th} approximation is good, $\mathcal{H}^{(m)}$ is small and therefore the minimum capital Λ_0 also decreases.

8.2.1 PROOF OF LEMMA 11

Since the posterior variance only decreases with more observations, we can upper bound $\kappa'(x, x)$ for any $x \in A$ by considering its posterior variance with only the s observations in A . Further the maximum variance within A occurs if we pick 2 points x_1, x_2 that are distance D apart and have all

observations at x_1 ; then x_2 has the highest posterior variance. Therefore, we will bound $\kappa'(x, x)$ for any $x \in A$ with $\kappa(x_2, x_2)$ in the above scenario. Let $\kappa_0 = \kappa(x, x)$ and $\kappa(x, x') = \kappa_0 \phi(\|x - x'\|_2)$, where $\phi(\cdot) \leq 1$ depends on the kernel. Denote the gram matrix in the scenario described above by $\Delta = \kappa_0 \mathbf{1}\mathbf{1}^\top + \eta^2 I$. Then using the Sherman-Morrison formula on the posterior variance (2),

$$\begin{aligned}
 \kappa'(x, x) &\leq \kappa'(x_2, x_2) = \kappa(x_2, x_2) - [\kappa(x_1, x_2)\mathbf{1}]^\top \Delta^{-1} [\kappa(x_1, x_2)\mathbf{1}] \\
 &= \kappa_0 - \kappa_0^2 \phi^2(D) \mathbf{1}^\top \left[\kappa_0 \mathbf{1}\mathbf{1}^\top + \eta^2 I \right]^{-1} \mathbf{1} \\
 &= \kappa_0 - \kappa_0 \phi^2(D) \mathbf{1}^\top \left[\frac{\kappa_0}{\eta^2} I - \frac{\left(\frac{\kappa_0}{\eta^2}\right)^2 \mathbf{1}\mathbf{1}^\top}{1 + \frac{\kappa_0}{\eta^2} s} \right] \mathbf{1} = \kappa_0 - \kappa_0 \phi^2(D) \left(\frac{\kappa_0}{\eta^2} s - \frac{\left(\frac{\kappa_0}{\eta^2}\right)^2 s^2}{1 + \frac{\kappa_0}{\eta^2} s} \right) \\
 &= \kappa_0 - \kappa_0 \phi^2(D) \frac{s}{\frac{\eta^2}{\kappa_0} + s} = \frac{1}{1 + \frac{\eta^2}{\kappa_0 s}} \left(\kappa_0 - \kappa_0 \phi^2(D) + \frac{\eta^2}{s} \right) \\
 &\leq \kappa_0 (1 - \phi^2(D)) + \frac{\eta^2}{s}.
 \end{aligned}$$

For the SE kernel $\phi^2(D) = \exp\left(\frac{-D^2}{2h^2}\right)^2 = \exp\left(\frac{-D^2}{h^2}\right) \leq 1 - \frac{D^2}{h^2}$. Plugging this into the bound above retrieves the first result with $C_{SE} = \kappa_0/h^2$. For the Matérn kernel we use a Lipschitz constant L_{Mat} of ϕ . Then $1 - \phi^2(D) = (1 - \phi(D))(1 + \phi(D)) \leq 2(\phi(0) - \phi(D)) \leq 2L_{Mat}D$. We get the second result with $C_{Mat} = 2\kappa_0 L_{Mat}$. Since the SE kernel decays fast, we get a stronger result on its posterior variance which translates to a better bound in our theorems. \blacksquare

8.2.2 PROOF OF LEMMA 12

The first part of the proof mimics the arguments in Lemmas 5.6, 5.7 of [Srinivas et al. \(2010\)](#). By Assumption 2 and the union bound we can show,

$$\mathbb{P}\left(\forall m \in \{1, \dots, M\}, \forall i \in \{1, \dots, d\}, \forall x \in \mathcal{X}, \left| \frac{\partial f^{(m)}(x)}{\partial x_i} \right| < b \log\left(\frac{6Mad}{\delta}\right)\right) \geq 1 - \frac{\delta}{6}.$$

Now we construct a discretisation F_t of \mathcal{X} of size $(\nu_t)^d$ such that we have for all $x \in \mathcal{X}$, $\|x - [x]_t\|_1 \leq rd/\nu_t$. Here $[x]_t$ is the closest point to x in the discretisation. (Note that this is different from the discretisation appearing in Theorem 7 even though we have used the same notation). By choosing $\nu_t = t^2 brd \sqrt{6Mad/\delta}$ and using the above we have

$$\forall x \in \mathcal{X}, \quad |f^{(m)}(x) - f^{(m)}([x]_t)| \leq b \log(6Mad/\delta) \|x - [x]_t\|_1 \leq 1/t^2 \quad (20)$$

for all $f^{(m)}$'s with probability $> 1 - \delta/6$.

Noting that $\beta_t \geq 2 \log(M|F_t|\pi^2 t^2/2\delta)$ for the given choice of ν_t we have the following with probability $> 1 - \delta/3$.

$$\forall t \geq 1, \forall m \in \{1, \dots, M\}, \forall a \in F_t, \quad |f^{(m)}(a) - \mu_{t-1}^{(m)}(a)| \leq \beta_t^{1/2} \sigma_{t-1}^{(m)}(a). \quad (21)$$

The proof mimics that of Lemma 9 using the same conditioning argument. However, instead of a fixed set over all t , we change the set at which we have confidence based on the discretisation.

Similarly we can show that with probability $> 1 - \delta/3$ we also have confidence on the decisions x_t at all time steps. Precisely,

$$\forall t \geq 1, \forall m \in \{1, \dots, M\}, \quad |f^{(m)}(x_t) - \mu_{t-1}^{(m)}(x_t)| \leq \beta_t^{1/2} \sigma_{t-1}^{(m)}(x_t). \quad (22)$$

Using (20),(21) and (22) the following statements hold with probability $> 1 - 5\delta/6$. First we can upper bound f_\star by,

$$f_\star \leq f^{(m)}(x_\star) + \zeta^{(m)} \leq f^{(m)}([x_\star]_t) + \zeta^{(m)} + \frac{1}{t^2} \leq \varphi_t^{(m)}([x_\star]_t) + \frac{1}{t^2}. \quad (23)$$

Since the above holds for all m , we have $f_\star \leq \varphi_t([x_\star]_t) + 1/t^2$. Now, using similar calculations as (12) we bound $\Delta^{(m)}(x_t)$.

$$\begin{aligned} \Delta^{(m)}(x_t) &= f_\star - f^{(m)}(x_t) - \zeta^{(m)} \\ &\leq \varphi_t([x_\star]_t) + \frac{1}{t^2} - f^{(m)}(x_t) - \zeta^{(m)} \leq \varphi_t(x_t) - f^{(m)}(x_t) - \zeta^{(m)} + \frac{1}{t^2} \\ &\leq \varphi_t^{(m)}(x_t) - \mu_{t-1}^{(M)}(x_t) + \beta_t^{1/2} \sigma_{t-1}^{(M)}(x_t) - \zeta^{(m)} + \frac{1}{t^2} \leq 2\beta_t^{1/2} \sigma_{t-1}^{(M)}(x_t) + \frac{1}{t^2}. \end{aligned} \quad \blacksquare$$

8.2.3 PROOF OF LEMMA 13

First, we will invoke the same discretisation used in the proof of Lemma 12 via which we have $\varphi_t([x_\star]_t) \geq f_\star - 1/t^2$ (23). (Therefore, Lemma 13 holds only with probability $> 1 - \delta/6$, but this event has already been accounted for in Lemma 12.) Let $b_{i,n,t} = \operatorname{argmax}_{x \in A_{i,n}} \varphi_t(x)$ be the maximiser of the upper confidence bound in $A_{i,n}$ at time t . Now using the relaxation $x_t \in A_{i,n} \implies \varphi_t(b_{i,n,t}) > \varphi_t([x_\star]_t) \implies \varphi_t^{(m)}(b_{i,n,t}) > f_\star - 1/t^2$ and proceeding,

$$\begin{aligned} \mathbb{P}(T_n^{(>m)}(A_{i,n}) > u) &\leq \mathbb{P}(\exists t : u+1 \leq t \leq n, \varphi_t^{(m)}(b_{i,n,t}) > f_\star - 1/t^2 \wedge \\ &\quad \beta_t^{1/2} \sigma_{t-1}^{(m)}(b_{i,n,t}) < \gamma^{(m)}) \quad (24) \\ &\leq \sum_{t=u+1}^n \mathbb{P}(\mu_{t-1}^{(m)}(b_{i,n,t}) - f^{(m)}(b_{i,n,t}) > \Delta^{(m)}(b_{i,n,t}) - \beta_t^{1/2} \sigma_{t-1}^{(m)}(b_{i,n,t}) - 1/t^2 \wedge \\ &\quad \beta_t^{1/2} \sigma_{t-1}^{(m)}(b_{i,n,t}) < \gamma^{(m)}) \\ &\leq \sum_{t=u+1}^n \mathbb{P}(\mu_{t-1}^{(m)}(b_{i,n,t}) - f^{(m)}(b_{i,n,t}) > (\rho-1)\beta_t^{1/2} \sigma_{t-1}^{(m)}(b_{i,n,t}) - 1/t^2) \\ &\leq \sum_{t=u+1}^n \mathbb{P}_{Z \sim \mathcal{N}(0,1)}(Z > (\rho_0-1)\beta_t^{1/2}) \leq \sum_{t=u+1}^n \frac{1}{2} \exp\left(-\frac{(\rho_0-1)^2}{2} \beta_t\right) \\ &\leq \frac{1}{2} \left(\frac{\delta}{M\pi^2}\right)^{(\rho_0-1)^2} \sum_{t=u+1}^n t^{-(\rho_0-1)^2(2+2d)} \leq \frac{\delta}{M\pi^2} u^{-(\rho_0-1)^2(2+2d)+1} \leq \frac{\delta}{\pi^2} \frac{1}{u^{1+4/\alpha}}. \end{aligned}$$

In the second step we have rearranged the terms and used the definition of $\Delta^{(m)}(x)$. In the third step, as $A_{i,n} \subset \overline{\mathcal{J}}_{\max(\tau, \rho\gamma)}^{(m)}$, $\Delta^{(m)}(b_{i,n,t}) > \rho\gamma^{(m)} > \rho\beta_t^{1/2} \sigma_{t-1}^{(m)}(b_{i,n,t})$. In the fourth step we have used

the following facts, $t > u \geq \max\{3, (2(\rho - \rho_0)\eta)^{-2/3}\}$, $M\pi^2/2\delta > 1$ and $\sigma_{t-1}^{(m)}(b_{i,n,t}) > \eta/\sqrt{t}$ to conclude,

$$\begin{aligned} (\rho - \rho_0) \frac{\eta \sqrt{4 \log(t)}}{\sqrt{t}} > \frac{1}{t^2} &\implies (\rho - \rho_0) \cdot \sqrt{2 \log\left(\frac{M\pi^2 t^2}{2\delta}\right)} \cdot \frac{\eta}{\sqrt{t}} > \frac{1}{t^2} \\ &\implies (\rho - \rho_0) \beta_t^{1/2} \sigma_{t-1}^{(m)}(b_{i,n,t}) > \frac{1}{t^2}. \end{aligned}$$

In the seventh step of (24) we have bound the sum by an integral and used $\rho_0 \geq 2$ twice. Finally, the last step follows by $\rho_0 \geq 1 + \sqrt{(1 + 2/\alpha)/(1 + d)}$ and noting $M \geq 1$. ■

9. Conclusion

We introduced and studied the multi-fidelity bandit problem under Gaussian Process assumptions which builds on our work on multi-fidelity K -armed bandits (Kandasamy et al., 2016b). Our theorems demonstrate that MF-GP-UCB explores the space using the cheap lower fidelities, and uses the higher fidelity queries on successively smaller regions, hence achieving better regret than single fidelity strategies. Via experiments on synthetic functions, three hyper-parameter tuning tasks, and an astrophysical maximum likelihood estimation problem, we demonstrate the efficacy of our method and more generally, the utility of the multi-fidelity framework. Our Matlab implementation and experiments can be downloaded from github.com/kirthevasank/mf-gp-ucb.

Going forward we wish to study multi-fidelity optimisation under different model assumptions, and extend the algorithm when we have to deal with approximations from structured fidelity spaces.

Appendix

Appendix A. Addendum to Experiments

A.1 Some Implementation Details of other Baselines

For MF-NAIVE we limited the number of first fidelity evaluations to $\max\left(\frac{1}{2} \frac{\Lambda}{\lambda^{(1)}}, 500\right)$ where Λ was the total budget used in the experiment. The 500 limit was set to avoid unnecessary computation – for all of these problems, 500 queries are not required to find the maximum. While there are other methods for multi-fidelity optimisation (discussed under Related Work) none of them had made their code available nor were their methods straightforward to implement - this includes MF-SKO.

A straightforward way to incorporate lower fidelity information to GP-UCB and EI is to share the same kernel parameters. This way, the kernel κ can be learned by jointly maximising the marginal likelihood. While the idea seems natural, we got mixed results in practice. On some problems this improved the performance of all GP methods (including MF-GP-UCB), but on others all performed poorly. One explanation is that while lower fidelities approximate function values, they are not always best described by the same kernel. The results presented do not use lower fidelities to learn κ as it was more robust. For MF-GP-UCB, each $\kappa^{(m)}$ was learned independently using only the queries at fidelity m .

In addition to the baselines presented in the figures, we also compared our method to the following methods. The first two are single fidelity and the last two are multi-fidelity methods.

- The probability of improvement (PI) criterion for BO (Brochu et al., 2010). We found that in general either GP-UCB or EI performed better.
- Querying uniformly at random at the highest fidelity and taking the maximum. On all problems this performed worse than other methods.
- A variant of MF-NAIVE where instead of GP-UCB we queried at the first fidelity uniformly at random. On some problems this did better than querying with GP-UCB, probably since unlike GP-UCB it was not stuck at the maximum of $f^{(1)}$. However, generally it performed worse.
- The multi-fidelity method from Forrester et al. (2007) also based on GPs. We found that this method did not perform as desired: in particular, it barely queried beyond the first fidelity.

A.2 Description of Synthetic Experiments

The following are the descriptions of the synthetic functions used. The first three functions and their approximations were taken from Xiong et al. (2013).

Currin exponential function: The domain is the two dimensional unit cube $\mathcal{X} = [0, 1]^2$. The second and first fidelity functions are,

$$f^{(2)}(x) = \left(1 - \exp\left(\frac{-1}{2x_2}\right)\right) \left(\frac{2300x_1^3 + 1900x_1^2 + 2092x_1 + 60}{100x_1^3 + 500x_1^2 + 4x_1 + 20}\right),$$

$$f^{(1)}(x) = \frac{1}{4}f^{(2)}(x_1 + 0.05, x_2 + 0.05) + \frac{1}{4}f^{(2)}(x_1 + 0.05, \max(0, x_2 - 0.05)) + \frac{1}{4}f^{(2)}(x_1 - 0.05, x_2 + 0.05) + \frac{1}{4}f^{(2)}(x_1 - 0.05, \max(0, x_2 - 0.05)).$$

Park function: The domain is $\mathcal{X} = [0, 1]^4$. The second and first fidelity functions are,

$$f^{(2)}(x) = \frac{x_1}{2} \left(\sqrt{1 + (x_2 + x_3^2) \frac{x_4}{x_1^2}} - 1 \right) + (x_1 + 3x_4) \exp(1 + \sin(x_3)),$$

$$f^{(1)}(x) = \left(1 + \frac{\sin(x_1)}{10}\right) f^{(2)}(x) - 2x_1^2 + x_2^2 + x_3^2 + 0.5.$$

Borehole function: The second and first fidelity functions are,

$$f^{(2)}(x) = \frac{2\pi x_3(x_4 - x_6)}{\log(x_2/x_1) \left(1 + \frac{2x_7x_3}{\log(x_2/x_1)x_1^2x_8} + \frac{x_3}{x_5}\right)},$$

$$f^{(1)}(x) = \frac{5x_3(x_4 - x_6)}{\log(x_2/x_1) \left(1.5 + \frac{2x_7x_3}{\log(x_2/x_1)x_1^2x_8} + \frac{x_3}{x_5}\right)}.$$

The domain of the function is $[0.05, 0.15; 100, 50K; 63.07K, 115.6K; 990, 1110; 63.1, 116; 700, 820; 1120, 1680; 9855, 12045]$. We first linearly transform the variables to lie in $[0, 1]^8$.

Hartmann-3D function: The M^{th} fidelity function is $f^{(M)}(x) = \sum_{i=1}^4 \alpha_i \exp\left(-\sum_{j=1}^3 A_{ij}(x_j - P_{ij})^2\right)$ where $A, P \in \mathbb{R}^{4 \times 3}$ are fixed matrices given below and $\alpha = [1.0, 1.2, 3.0, 3.2]$. For the

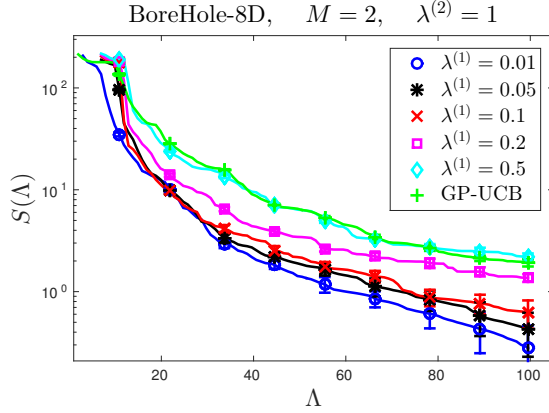


Figure 9: The performance of our implementation of MF-GP-UCB for different values of $\lambda^{(1)}$ in the 2 fidelity Borehole experiment. Our implementation uses the techniques and heuristics described in Section 6. In all experiments we used $\lambda^{(2)} = 1$. We have also shown the curve for GP-UCB for reference.

lower fidelities we use the same form except changing α to $\alpha^{(m)} = \alpha + (M - m)\delta$ where $\delta = [0.01, -0.01, -0.1, 0.1]$ and $M = 3$. The domain is $\mathcal{X} = [0, 1]^3$.

$$A = \begin{bmatrix} 3 & 10 & 30 \\ 0.1 & 10 & 35 \\ 3 & 10 & 30 \\ 0.1 & 10 & 35 \end{bmatrix}, \quad P = 10^{-4} \times \begin{bmatrix} 3689 & 1170 & 2673 \\ 4699 & 4387 & 7470 \\ 1091 & 8732 & 5547 \\ 381 & 5743 & 8828 \end{bmatrix}$$

Hartmann-6D function: The 6-D Hartmann function takes the same form as the 3-D case except $A, P \in \mathbb{R}^{4 \times 6}$ are as given below. We use the same modifications as above to obtain the lower fidelities using $M = 4$.

$$A = \begin{bmatrix} 10 & 3 & 17 & 3.5 & 1.7 & 8 \\ 0.05 & 10 & 17 & 0.1 & 8 & 14 \\ 3 & 3.5 & 1.7 & 10 & 17 & 8 \\ 17 & 8 & 0.05 & 10 & 0.1 & 14 \end{bmatrix}, \quad P = 10^{-4} \times \begin{bmatrix} 1312 & 1696 & 5569 & 124 & 8283 & 5886 \\ 2329 & 4135 & 8307 & 3736 & 1004 & 9991 \\ 2348 & 1451 & 3522 & 2883 & 3047 & 6650 \\ 4047 & 8828 & 8732 & 5743 & 1091 & 381 \end{bmatrix}$$

A.3 Additional Experiments

Cost of the Approximation: In Figure 9 we test our implementation on the 2-fidelity Borehole experiment for different costs for the approximation. We fixed $\lambda^{(2)} = 1$ and varied $\lambda^{(1)}$ between 0.01 to 0.5. As $\lambda^{(1)}$ increases, the performance worsens as expected. At $\lambda^{(1)} = 0.5$ it is indistinguishable from GP-UCB as the overhead of managing 2 fidelities becomes significant when compared to the improvements of using the approximation.

Bad Approximations: It is natural to ask how MF-GP-UCB performs with bad approximations at lower fidelities. We found that our implementation with the heuristics suggested in Section 6 to be quite robust. We demonstrate this using the Currin exponential function, but using the negative of $f^{(2)}$ as the first fidelity approximation, i.e. $f^{(1)}(x) = -f^{(2)}(x)$. Figure 10 illustrates $f^{(1)}, f^{(2)}$ and gives the simple regret $S(\Lambda)$. Understandably, it loses to the single fidelity methods since the first fidelity queries are wasted and it spends some time at the second fidelity recovering from the bad approximation. However, it eventually is able to achieve low regret.

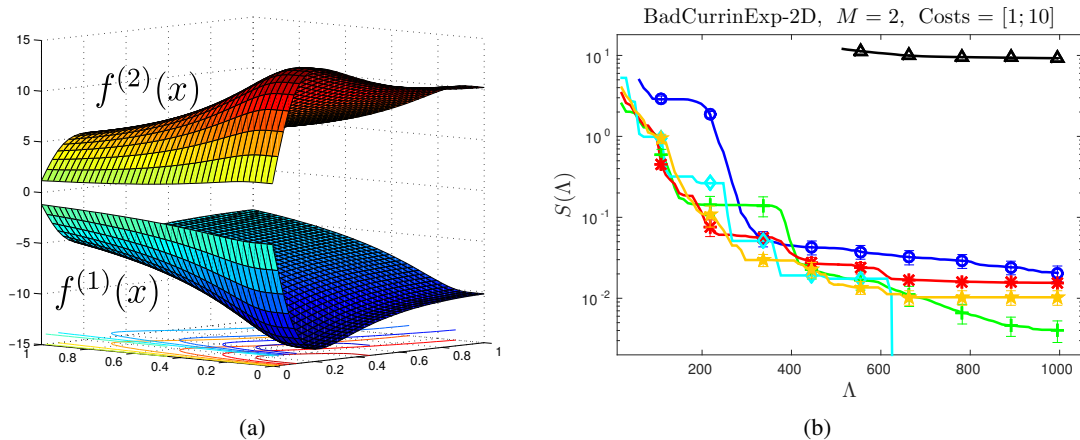


Figure 10: (a): the functions used in the Bad Currin Exponential experiment where $f^{(1)} = -f^{(2)}$. (b): the simple regret for this experiment. See caption under Figure 6 for more details.

Appendix B. Other Material

B.1 Some Ancillary Results

The following results were used in our analysis. The first is a standard Gaussian concentration result and the second is an expression for the Information Gain in a GP from Srinivas et al. (2010).

Lemma 14 (Gaussian Concentration) *Let $Z \sim \mathcal{N}(0, 1)$. Then $\mathbb{P}(Z > \epsilon) \leq \frac{1}{2} \exp(-\epsilon^2/2)$.*

Lemma 15 (Mutual Information in GP, Srinivas et al. (2010), Lemma 5.3) *Let $f \sim \mathcal{GP}(\mathbf{0}, \kappa)$, $f : \mathcal{X} \rightarrow \mathbb{R}$ and we observe $y = f(x) + \epsilon$ where $\epsilon \sim \mathcal{N}(0, \eta^2)$. Let A be a finite subset of \mathcal{X} and f_A, y_A be the function values and observations on this set respectively. Using the basic Gaussian properties it can be shown that the mutual information $I(y_A; f_A)$ is,*

$$I(y_A; f_A) = \frac{1}{2} \sum_{t=1}^n \log(1 + \eta^{-2} \sigma_{t-1}^2(x_t)).$$

where σ_{t-1}^2 is the posterior GP variance after observing the first $t - 1$ points.

We conclude this section with the following comment on our assumptions in Section 2.

Remark 16 (Validity of the Assumption A2) We argue that when the functions $f^{(m)}$ are sampled from $\mathcal{GP}(\mathbf{0}, \kappa)$, assumption A2, i.e. $\|f^{(M)} - f^{(m)}\|_\infty \leq \zeta^{(m)} \forall m$, occurs with positive probability. Then, a generative mechanism would repeatedly sample the $f^{(m)}$'s from the GP and output them when the constraints are satisfied. Since $f^{(M)} - f^{(m)} \sim \mathcal{GP}(\mathbf{0}, 2\kappa)$ is a GP, it is sufficient to show that the supremum of this GP is bounded by $\zeta^{(m)}$ with positive probability. This argument is straightforward when \mathcal{X} is discrete. For continuous \mathcal{X} , the claim is true for well behaved kernels. For instance, using Assumption 2 we can establish a high probability bound on the Lipschitz constant of the GP sample $f^{(M)} - f^{(m)}$. Since for a given $x \in \mathcal{X}$, $\mathbb{P}(-\zeta^{(m)} < f^{(M)}(x) - f^{(m)}(x) < \zeta^{(m)})$ is positive, we just need to set the Lipschitz constant to be $\zeta^{(m)}/\text{diam}(\mathcal{X})$.

B.2 A Table of Notations and Abbreviations

The following table summarises the notation and abbreviations used in the manuscript. The table continues to multiple pages.

Notation	Description
M	The number of fidelities.
$f, f^{(m)}$	The payoff function and its m^{th} fidelity approximation. $f^{(M)} = f$.
Λ	Λ typically denotes the capital of some resource which is expended upon each evaluation of at any fidelity.
$\lambda^{(m)}$	The cost, i.e. amount of capital expended, of querying at fidelity m .
N	The random number of queries at any fidelity within capital Λ . $N = \max\{n \geq 1 : \sum_{t=1}^n \lambda^{(m_t)} \leq \Lambda\}$
\mathcal{X}	The domain over which we are optimising f .
x_*, f_*	The optimum point and value of the M^{th} fidelity function.
\bar{A}	The complement of a set $A \subset \mathcal{X}$. $\bar{A} = \mathcal{X} \setminus A$.
$ A $	The cardinality of a set $A \subset \mathcal{X}$ if it is countable.
\vee, \wedge	Logical <i>Or</i> and <i>And</i> respectively.
$\lesssim, \gtrsim, \asymp$	Inequalities and equality ignoring constant terms.
q_t, r_t	The instantaneous reward and regret respectively. $q_t = f^{(M)}(x_t)$ if $m_t = M$ and $-\infty$ if $m_t \neq M$. $r_t = f_* - q_t$.
$S(\Lambda)$	The simple regret after spending capital Λ . $S(\Lambda) = f_* - \min_{t=1, \dots, N} f(x_t)$.
$\zeta^{(m)}$	The bound on the maximum difference between $f^{(m)}$ and $f^{(M)}$, $\ f^{(M)} - f^{(m)}\ _\infty \leq \zeta^{(m)}$.
$\mu_t^{(m)}$	The mean of the m^{th} fidelity GP $f^{(m)}$ conditioned on $\mathcal{D}_t^{(m)}$ at time t .
$\kappa_t^{(m)}$	The covariance of the m^{th} fidelity GP $f^{(m)}$ conditioned on $\mathcal{D}_t^{(m)}$ at time t .
$\sigma_t^{(m)}$	The standard deviation of the m^{th} fidelity GP $f^{(m)}$ conditioned on $\mathcal{D}_t^{(m)}$ at time t .
x_t, y_t	The queried point and observation at time t .
m_t	The queried fidelity at time t .
$\mathcal{D}_n^{(m)}$	The set of queries at the m^{th} fidelity until time n $\{(x_t, y_t)\}_{t:m_t=m}$.
β_t	The coefficient trading off exploration and exploitation in the UCB. See Theorems 6 and 7.
$\varphi_t^{(m)}(x)$	The upper confidence bound (UCB) provided by the m^{th} fidelity on $f^{(M)}(x)$. $\varphi_t^{(m)}(x) = \mu_{t-1}^{(m)}(x) + \beta_t^{1/2} \sigma_{t-1}^{(m)}(x) + \zeta^{(m)}$.
$\varphi_t(x)$	The combined UCB provided by all fidelities on $f^{(M)}(x)$. $\varphi_t(x) = \min_m \varphi_t^{(m)}(x)$.
$\gamma^{(m)}$	The parameter in MF-GP-UCB for switching from the m^{th} fidelity to the $(m+1)^{\text{th}}$.
\tilde{R}_n	The M^{th} fidelity cumulative regret after n rounds. See (7)
$T_n^{(m)}(A)$	The number of queries at fidelity m in subset $A \subset \mathcal{X}$ until time n .
$T_n^{(>m)}(A)$	Number of queries at fidelities greater than m in any subset $A \subset \mathcal{X}$ until time n .
n_Λ	Number of plays by a strategy querying only at fidelity M within capital Λ . $n_\Lambda = \lfloor \Lambda / \lambda^{(M)} \rfloor$.

$\Psi_n(A)$	The maximum information gain of a set $A \subset \mathcal{X}$ after n queries in A . See Definition 1.
$\Delta^{(m)}(x)$	$\Delta^{(m)}(x) = f_\star - f^{(m)} - \zeta^{(m)}$.
$\mathcal{J}_\eta^{(m)}$	The points in \mathcal{X} whose $f^{(m)}$ value is within $\zeta^{(m)} + \eta$ of the optimum f_\star . $\mathcal{J}_\eta^{(m)} = \{x \in \mathcal{X}; \Delta^{(m)}(x) \leq \eta\}$.
$\mathcal{H}^{(m)}$	$(\mathcal{H}^{(m)})_{m=1}^M$ is a partitioning of \mathcal{X} in the discrete case. See Equation (5). The analysis of MF-GP-UCB hinges on these partitioning.
$\widehat{\mathcal{H}}^{(m)}, \widetilde{\mathcal{H}}^{(m)}$	The arms “above”/“below” $\mathcal{H}^{(m)}$. $\widehat{\mathcal{H}}^{(m)} = \bigcup_{\ell=m+1}^M \mathcal{H}^{(\ell)}$, $\widetilde{\mathcal{H}}^{(m)} = \bigcup_{\ell=1}^{m-1} \mathcal{H}^{(\ell)}$.
$\mathcal{H}_\tau^{(m)}$	$(\mathcal{H}_\tau^{(m)})_{m=1}^M$ is a partitioning of \mathcal{X} in the continuous and compact. See Equation (6). The analysis of MF-GP-UCB hinges on these partitioning.
$\mathcal{H}_{\tau,n}^{(m)}$	An additional n -dependent inflation of $\mathcal{H}_\tau^{(m)}$. See paragraph under equation (6).
$\widehat{\mathcal{H}}_\tau^{(m)}, \widetilde{\mathcal{H}}_\tau^{(m)}$	The arms “above”/“below” $\mathcal{H}_\tau^{(m)}$. $\widehat{\mathcal{H}}_\tau^{(m)} = \bigcup_{\ell=m+1}^M \mathcal{H}_\tau^{(\ell)}$, $\widetilde{\mathcal{H}}_\tau^{(m)} = \bigcup_{\ell=1}^{m-1} \mathcal{H}_\tau^{(\ell)}$.
\mathcal{X}_g	The good set for $M = 2$ fidelity problems. $\mathcal{X}_g = \{x \in \mathcal{X}; f_\star - f^{(1)}(x) \leq \zeta^{(1)}\}$.
$\mathcal{X}_{g,\rho}$	The inflated good set for MF-GP-UCB. $\mathcal{X}_{g,\rho} = \{x; f_\star - f^{(1)}(x) \leq \zeta^{(1)} + \rho\gamma\}$.
$\Omega_\varepsilon(A)$	The ε -covering number of a subset $A \subset \mathcal{X}$ in the $\ \cdot\ _2$ metric.
Λ_0	The minimum capital that needs to be expended before the bound on $S(\Lambda)$ hold in Theorem 6 and 7.
Abbreviation	Description
UCB	Upper Confidence Bound
BO	Bayesian Optimisation
GP-UCB	Gaussian Process Upper Confidence Bound (Srinivas et al., 2010)
MF-GP-UCB	Multi-fidelity Gaussian Process Upper Confidence Bound
EI	(Gaussian Process) Expected Improvement (Jones et al., 1998)
MF-SKO	Multi-fidelity Sequential Kriging Optimisation (Huang et al., 2006)
MF-NAIVE	Naive multi-fidelity method described in Section 7.
DiRect	DIViding RECTangles (Jones et al., 1993)
SE	Squared Exponential (in reference to the kernel)

Acknowledgments

We wish to thank Bharath Sriperumbudur for the helpful email discussions. This research was partly funded by DOE grant DESC0011114.

References

Alekh Agarwal, John C Duchi, Peter L Bartlett, and Clement Levrard. Oracle inequalities for computationally budgeted model selection. In *COLT*, 2011.

Peter Auer. Using Confidence Bounds for Exploitation-exploration Trade-offs. *J. Mach. Learn. Res.*, 2003.

- E. Brochu, V. M. Cora, and N. de Freitas. A Tutorial on Bayesian Optimization of Expensive Cost Functions, with Application to Active User Modeling and Hierarchical RL. *CoRR*, 2010.
- Sébastien Bubeck and Nicolò Cesa-Bianchi. Regret analysis of stochastic and nonstochastic multi-armed bandit problems. *Foundations and Trends in Machine Learning*, 2012.
- Mark Cutler, Thomas J. Walsh, and Jonathan P. How. Reinforcement Learning with Multi-Fidelity Simulators. In *ICRA*, 2014.
- V. Dani, T. P. P. Hayes, and S. M. Kakade. Stochastic Linear Optimization under Bandit Feedback. In *COLT*, 2008.
- T. M. Davis et al. Scrutinizing Exotic Cosmological Models Using ESSENCE Supernova Data Combined with Other Cosmological Probes. *Astrophysical Journal*, 2007.
- Alexander I. J. Forrester, András Sóbester, and Andy J. Keane. Multi-fidelity optimization via surrogate modelling. *Proceedings of the Royal Society A: Mathematical, Physical and Engineering Science*, 2007.
- Subhashis Ghosal and Anindya Roy. Posterior consistency of Gaussian process prior for nonparametric binary regression”. *Annals of Statistics*, 2006.
- José Miguel Hernández-Lobato, Matthew W Hoffman, and Zoubin Ghahramani. Predictive Entropy Search for Efficient Global Optimization of Black-box Functions. In *NIPS*, 2014.
- D. Huang, T.T. Allen, W.I. Notz, and R.A. Miller. Sequential kriging optimization using multiple-fidelity evaluations. *Structural and Multidisciplinary Optimization*, 2006.
- D. R. Jones, C. D. Perttunen, and B. E. Stuckman. Lipschitzian Optimization Without the Lipschitz Constant. *J. Optim. Theory Appl.*, 1993.
- Donald R. Jones, Matthias Schonlau, and William J. Welch. Efficient global optimization of expensive black-box functions. *J. of Global Optimization*, 1998.
- Kirthevasan Kandasamy and Yaoliang Yu. Additive Approximations in High Dimensional Nonparametric Regression via the SALSA. In *ICML*, 2016.
- Kirthevasan Kandasamy, Jeff Schenider, and Barnabás Póczos. High Dimensional Bayesian Optimisation and Bandits via Additive Models. In *International Conference on Machine Learning*, 2015.
- Kirthevasan Kandasamy, Gautam Dasarathy, Junier Oliva, Jeff Schenider, and Barnabás Póczos. Gaussian Process Bandit Optimisation with Multi-fidelity Evaluations. In *Advances in Neural Information Processing Systems*, 2016a.
- Kirthevasan Kandasamy, Gautam Dasarathy, Jeff Schneider, and Barnabas Póczos. The Multi-fidelity Multi-armed Bandit. In *NIPS*, 2016b.
- Kirthevasan Kandasamy, Gautam Dasarathy, Jeff Schneider, and Barnabas Póczos. Multi-fidelity Bayesian Optimisation with Continuous Approximations. *arXiv preprint arXiv:1703.06240*, 2017.

- K. Kawaguchi, L. P. Kaelbling, and T. Lozano-Pérez. Bayesian Optimization with Exponential Convergence. In *NIPS*, 2015.
- S. Kirkpatrick, C. D. Gelatt, and M. P. Vecchi. Optimization by simulated annealing. *SCIENCE*, 1983.
- A. Klein, S. Bartels, S. Falkner, P. Hennig, and F. Hutter. Towards efficient Bayesian Optimization for Big Data. In *BayesOpt*, 2015.
- R. Martinez-Cantin, N. de Freitas, A. Doucet, and J. Castellanos. Active Policy Learning for Robot Planning and Exploration under Uncertainty. In *Proceedings of Robotics: Science and Systems*, 2007.
- Jonas Mockus. Application of Bayesian approach to numerical methods of global and stochastic optimization. *Journal of Global Optimization*, 1994.
- R. Munos. Optimistic Optimization of Deterministic Functions without the Knowledge of its Smoothness. In *NIPS*, 2011.
- D. Parkinson, P. Mukherjee, and A. R Liddle. A Bayesian model selection analysis of WMAP3. *Physical Review*, 2006.
- C.E. Rasmussen and C.K.I. Williams. *Gaussian Processes for Machine Learning*. UPG Ltd, 2006.
- Herbert Robbins. Some aspects of the sequential design of experiments. *Bulletin of the American Mathematical Society*, 1952.
- A Sabharwal, H Samulowitz, and G Tesauro. Selecting near-optimal learners via incremental data allocation. In *AAAI*, 2015.
- MW. Seeger, SM. Kakade, and DP. Foster. Information Consistency of Nonparametric Gaussian Process Methods. *IEEE Transactions on Information Theory*, 2008.
- J. Snoek, H. Larochelle, and R. P Adams. Practical Bayesian Optimization of Machine Learning Algorithms. In *NIPS*, 2012.
- Niranjan Srinivas, Andreas Krause, Sham Kakade, and Matthias Seeger. Gaussian Process Optimization in the Bandit Setting: No Regret and Experimental Design. In *ICML*, 2010.
- Kevin Swersky, Jasper Snoek, and Ryan P Adams. Multi-task bayesian optimization. In *NIPS*, 2013.
- W. R. Thompson. On the Likelihood that one Unknown Probability Exceeds Another in View of the Evidence of Two Samples. *Biometrika*, 1933.
- Chris Urmson, Joshua Anhalt, Drew Bagnell, Christopher Baker, Robert Bittner, MN Clark, John Dolan, Dave Duggins, Tugrul Galatali, Chris Geyer, et al. Autonomous Driving in Urban Environments: Boss and the Urban Challenge. *Journal of Field Robotics*, 2008.
- Vladimir Naumovich Vapnik and Vladimir Vapnik. *Statistical learning theory*. Wiley New York, 1998.

Paul A. Viola and Michael J. Jones. Rapid Object Detection using a Boosted Cascade of Simple Features. In *Computer Vision and Pattern Recognition*, 2001.

Shifeng Xiong, Peter Z. G. Qian, and C. F. Jeff Wu. Sequential design and analysis of high-accuracy and low-accuracy computer codes. *Technometrics*, 2013.

C. Zhang and K. Chaudhuri. Active Learning from Weak and Strong Labelers. In *NIPS*, 2015.